UMTRI-86-53

CHARACTERIZATION OF THE THORAX
VIA MECHANICAL IMPEDANCE

Nabih Alem
University of Michigan
Transportation Research Institute
Ann Arbor, Michigan 48109

Said Nakhla
Bioengineering Center
Wayne State University
Detroit, Michigan 48202

TECHNICAL SUPPLEMENTAL REPORT
November 1986

1. Report No.	2. Government Accession No.	3. Recipient's Catalog No.

4. Title and Subtitle	5. Report Date
CHARACTERIZATION OF THE THORAX VIA MECHANICAL IMPEDANCE	November 1986
	6. Performing Organization Code

7. Author's)	8. Performing Organization Report No.
Nabih M. Alem and Said Nakhla*	UMTRI-86-53

9. Performing Organization Name and Address	10. Work Unit No. (TRAIS)
The University of Michigan Transportation Research Institute 2901 Baxter Road Ann Arbor, Michigan 48109-2150	
	11. Contract or Grant No.
	DTNH22-83-C-07005

12. Sponsoring Agency Name and Address	13. Type of Report and Period Covered
U.S. Department of Transportation National Highway Traffic Safety Administration Washington, D.C. 20590	TECHNICAL SUPPLEMENTAL REPORT†
	14. Sponsoring Agency Code

15. Supplementary Notes
*Work performed under subcontract to Wayne State University, Detroit, Michigan.

16. Abstract

A pilot study was undertaken as part of the biomechanical data analysis task of the AATD project to characterize the thorax as a mechanical system. Two distinct approaches were used. In the first, the mechanical impedance transfer functions were determined using frequency domain techniques. In the second, the Lobdell lumped-parameter chest model was assumed and parameter values were determined.

The study used experimentally generated signals from four chest impact tests to demonstrate the procedures and to: (1) produce classical impedance curves (CICs) for a linear version of the Lobdell chest model, (2) perform a parametric study of the Lobdell model in order to understand the effects of each parameter on the shape of the impedance curve, (3) generate impact impedance curves from four impacts, and (4) subject the Lobdell model to simulated impacts and apply the impact impedance technique to the simulated response in order to verify the validity of the identification process.

†Supplements AATD Task E-F final report: Melvin, J.W.; King, A.I.; and Alem, N.M. *AATD system technical characteristics, design concepts, and trauma assessment criteria.* The University of Michigan, Department of Mechanical Engineering and Applied Mechanics, Ann Arbor.

17. Key Words	18. Distribution Statement
Impact Response Thorax Mechanical Impedance	Unlimited

19. Security Classif. (of this report)	20. Security Classif. (of this page)	21. No. of Pages	22. Price
None	None	71	

CONTENTS

LIST OF FIGURES

RESEARCH OVERVIEW

BACKGROUND AND OBJECTIVES

An essential first step in the development of a biomechanically faithful and anthropomorphic test device is the impact response characterization of the anatomical segments of the human body. The goal of this step is to provide the designer with a set of mechanical descriptors to serve as a starting point in the design process, and with a set of impact response corridors to serve as an end point in the testing and evaluation process.

The foundation for this analysis must necessarily be the biomechanical data obtained from volunteers, cadavers, and animal tests over the last two decades. Since the bulk of the biomechanical data base available to the AATD project consisted of acceleration signals from cadaver impact tests, it was logical to develop methods and procedures that rely on acceleration impact response to identify the mechanical properties of various body segments. Furthermore, accelerometers seem to be the most reliable type of transducers that can be implanted in a mechanical ATD, so that the methodology used for characterization of human response should lend itself to direct or indirect implementation during the verification phase of the ATD biofidelity and during its ultimate deployment as a test device.

A pilot study was undertaken as part of the biomechanical data analysis task of the AATD project to characterize the thorax as a mechanical system. The thorax was selected for several reasons. First, based on programmatic considerations, the chest was given the highest priority in the order of data analysis and development of ATD specifications. Second, acceleration signals from thoracic impact tests were the most common signals included in the AATD biomechanical data base, thus providing the most suitable pool of signals for demonstrating the validity of the data analysis methods. Third, various characterization methods have been applied to thoracic impacts so that results from any new analysis procedures can be readily verified and/or critiqued.

DATA ANALYSIS METHODS

Two distinct approaches have been used to characterize the thorax. The first may be described as a black box approach, where the input–output relationship is derived directly from corresponding measurements. Examples of this method include transfer functions in the frequency domain such as impedance, spectral density, and auto- and cross-correlation functions. In the time domain, the characterization takes the form of impact response corridors given as functions of time. This approach is most useful during verification of dummy thorax biofidelity, but may also be used to identify the mechanical parameters of the system that produced the response.

The mechanical impedance method, employed at the University of Michigan Transportation Research Institute (UMTRI) for several years, uses transducer data only and film data are not needed. The method requires an *input* signal (e.g., impact force) and an *output* signal (e.g., acceleration response). No restriction is placed on the direction or location of either the input or output and, in some cases, the method may be generalized to produce a *transfer function* between any two measured signals affected by the mechanical properties of the impacted system. The transfer function is plotted as a function of

1

frequency. When mechanical impedance is the transfer function, system parameters such as mass, spring and damping constants may be inferred from the frequency plots.

Classically, mechanical impedances are defined for systems that are being excited by steady–state vibrations. Because the UMTRI technique derives these transfer functions from transient and short–lived impact responses, one may question the validity of any traditional interpretation based on non–traditional frequency responses. A full understanding of these impact impedance curves is therefore required before making traditional interpretations, or defining new principles that apply to this type of impedance curve.

The second system characterization method assumes, *a priori*, a model for the system and then attempts to identify the parameter values of the model from impact response of the actual system. The identification process may employ a trial–and–error method, or a least–squares algorithm which directly extracts the parameters that produce the best fit of the model response to the experimentally measured response.

Both methods were applied in a pilot study to characterize the chest as a mechanical system. The second method used force–deflection curves to extract spring, damping, and mass parameters of the chest. The procedure and results are described in the Task E–F final report in the AATD series of report.

The mechanical impedance technique was initially intended to be used on various body segments where only transducer data were available for analysis. However, due to changes in program priorities, further development and refinement of the method were abandoned. The objective of this report is to document the work that was performed in this area.

OUTLINE OF THE STUDY

The pilot study was conducted at the University of Michigan Transportation Research Institute (UMTRI) in cooperation with the staff of the Wayne State University (WSU) Bioengineering Center. Experimentally generated signals from four chest impact tests were selected from those available at the time to demonstrate the feasibility of the characterization methods. These included three pendulum frontal impact tests (76T053, 76T056, 76T059) and one pendulum side impact test (76T062). The selection was based on the availability and the quality of both transducer signals and digitized film because the same tests were to be used for demonstrating both the force–deflection method and the mechanical impedance technique.

In order to validate the second characterization method, it was applied to a system with known properties. The system selected was the Lobdell lumped–parameter chest model which has been widely used and shown to adequately simulate the chest impact behavior. The pilot study included the following impedance–related activities:

1. Produce classical impedance curves (CIC) for the linear version of the Lobdell model. This required rewriting of the impedance plotting program to overlay up to four impedance–frequency functions.

2. Perform a parametric study of the Lobdell linear model in order to understand and isolate the effects of each parameter on the shape of the impedance curve and to provide a basis for interpreting the impact impedance curves generated from actual measurements.

2

3. Generate impact impedance curves from the four selected chest impact tests, and attempt to isolate/identify from these curves the mechanical parameters of the chest.

4. Subject the Lobdell model to simulated impacts, and apply the impact impedance technique to the simulated response in order to verify the ability and validity of the identification process.

The last two sections of this report present the results of these activities. First, the classical impedance curves of the Lobdell model are presented. These are followed by the impact impedance results from the four tests and from the simulated impact of the Lobdell model, as outlined in tasks 3 and 4 above. For convenience to the reader, the conclusions and recommendations derived from these results are given on page 5.

CONCLUSIONS AND RECOMMENDATIONS

An impedance data analysis technique was proposed for characterizing the mechanical properties of the thorax. The method relies primarily on transducer signals recorded during impact and produces impedance curves. The technique was used and evaluated, producing the following conclusions and recommendations.

1. Linear lumped-parameter models of the chest can be easily studied in the frequency domain by using Network Analysis by Mechanical Impedance Techniques to produce Classical Impedance Curves. The lumped-parameter modeling and the CICs are basic tools for understanding the gross mechanical characteristics of the thorax.

2. Impact Impedance Curves, or IICs, can be produced from biomechanical impact testing. Limitations of the IICs stem from the sampling rate, the duration of the recorded signal, and the bandlimiting of the frequencies contained in the signals.

3. Simulations of IICs on a lumped-parameter model indicate that, except for the low-frequency end of the curves, the behavior is identical to the CICs of the same model. Thus, impact impedance analysis is a valid approach when reasonably accurate impact signals are used.

4. Consistent trends exhibited from three frontal impact test IICs indicate that the Lobdell configuration is not necessarily the most suitable lumped-parameter model for the thorax. However, since only three frontal tests were analyzed, no conclusive statement may be made at this stage.

5. The IICs are generally useful to determine damping characteristics, sternal mass, and natural frequencies in the 10- to 500-Hz range. Reading off values of spring constants and accurate determination of other numeric values remains difficult because of the spread of the overplotted curves.

6. The use of a postulated lumped-parameter model is essential in attempting to interpret the IICs. Other response signals, such as acceleration time-histories, should also guide the refinement of the postulated model.

7. When a sufficient number of tests are analyzed, statistical evaluation of the postulated model should yield more conclusive and convincing chest model configuration and numerical values.

8. When large deformations do not occur under impacts, such as head, knee, or pelvis impacts, the impedance method may be the only feasible technique for characterization of the mechanical properties of the impacted body part.

CONCLUSIONS AND RECOMMENDATIONS

CLASSICAL IMPEDANCE CURVES

When a mechanical system consisting of masses, springs, and dampers reaches steady-state response under forced vibration, the ratio of input force to the resulting velocity (both sinusoidal) is called the mechanical impedance of the system. This quantity is a complex function of frequency and of the masses, springs, and dampers of the system.

NETWORK REPRESENTATION

Figure 1* shows the impedances $Z(2)$ and mobilities $M(w) = 1/Z(w)$ of ideal mass, spring, and damper elements.

BASIC NETWORK REDUCTIONS

Basic elements (mass, spring, dashpot) are each represented as a block or branch between two nodes. The branches between the same two nodes are elements in parallel that may be reduced to a single equivalent impedance. Two branches connected end to end are elements in series and may be reduced to a single equivalent impedance between the two outside nodes. Finally, three elements connected in series to form a closed loop (a delta) may be converted to an open network by adding one node at the center of the delta and converting it to a Y-connection. These reductions are shown in Figure 2.

LINEAR LOBDELL MODEL NETWORK

The chest of the Lobdell model consists of masses M2 and M3, springs K23 and K24, and dashpots C23 and C43, as shown in Figure 3. The classical concept of impedance requires that the masses, springs, and damping constants to be time-invariant quantities. Thus, neither the non-linearity of K23, nor the bidirectionality of C23 can be allowed in the linear version of the chest model. Figure 4 is the network representation of this model, in which G is the ground node.

The driving point impedance of the model is the impedance between nodes 2 and G. The network is reduced to a single equivalent impedance by the following sequence of basic transformations.

a.	P23	=	Parallel	(K23,C23),	resulting in Figure 5(a)
b.	S23	=	Series	(K24,C24),	resulting in Figure 5(b)
c.	Q23	=	Parallel	(P23,S23),	resulting in Figure 5(c)
d.	S2G	=	Series	(Q23,M3),	resulting in Figure 5(d)
e.	Z2G	=	Parallel	(M2, S2G),	resulting in Figure 5(e)

This sequence of numerical computations is repeated at the desired spectrum of frequencies, resulting in the driving point impedance between M2 and Ground.

---

* Figures appear at the end of each section.

This numerical procedure avoids the error-prone and lengthy process of writing analytical expressions for the impedance, and more importantly, can be easily modified when there is a need to reconfigure the model by writing a different sequence of basic transformations.

Only one subroutine which makes the above sequence of calls was written. Other routines to perform basic conversions were lifted from the Network Analysis by Mechanical Impedance Techniques (NAMIT) at UMTRI.

PARAMETRIC CICs

Classical Impedance Curves (CICs) of the linear Lobdell model were generated. These were obtained by calling the subroutine described in the previous section at a spectrum of 400 frequencies at equal logarithmic intervals between 1 Hz and 10,000 Hz. A new impedance plotting program was written because the previously developed UMTRI impedance program was locked to 6400 Hz sampling rate and 100 msec signal length. The new plotting program allowed easy modifications of the frequency points where impedances are computed and plotted.
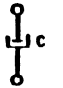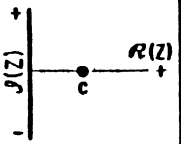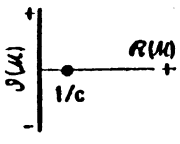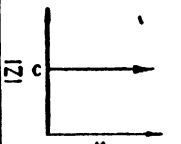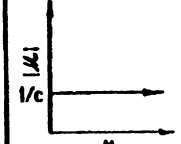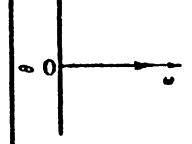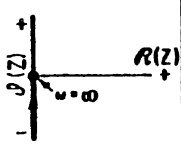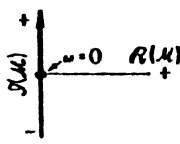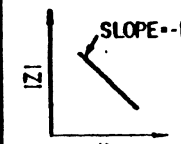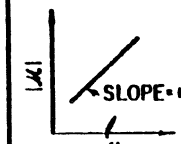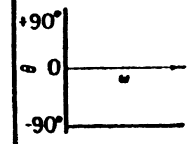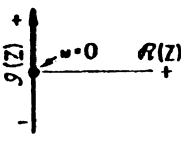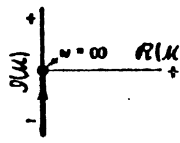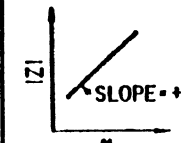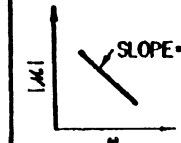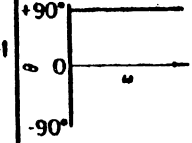
A parametric study was then conducted to understand the effects of varying the model's constants on the shape of the CIC. The results are shown in the six graphs of Figures 6 through 11.

As one would expect, varying the M2 and M3 changes the high- and low-frequency portions of the CIC, respectively. At high frequencies, the chest acts like a pure small mass M2 (Figure 6), while at low frequencies, the whole chest moves as a heavy mass, M2+M3, as shown in Figure 7. By increasing the value assigned to M3 (the chest mass), the resonance of the impedance curve is accentuated, but as expected, the natural frequency becomes lower. This natural frequency is not easily discerned from the base values of the Lobdell model, i.e., those assigned by Lobdell to represent the parameters of his model.

The next two parameters studied were the chest stiffness K23 and damping C23. These were constant values and not a bilinear spring and a bidirectional damping as specified in the original Lobdell model. Results for K23 variations are shown in Figure 8, and those for C23 are in Figure 9. Here again, the natural frequency is shifted to the right (higher) for higher K23 values. However, by varying the damping C23, the natural frequency does not change as long as the ratio K/M remains the same. From Figure 9, it is apparent that the natural frequency of the linear model is about 7 Hz. Furthermore, it is obvious that the shape of the CIC and its position on the impedance scale are extremely sensitive to the value assigned to C23 damping.

Finally, the series viscoelastic elements, K24 and C43, were varied. Results are shown in Figures 10 and 11. As indicated, there is only one curve on each graph. The CICs for all values of K24 and C43 are identical, indicating that these parameters have no effects on impedance curves, and perhaps suggesting their elimination from the chest model. However, further examination of the computer code that generated them, and a study of the effects of these constants on other responses, such as acceleration time-histories and force-deflections, are warranted before a final recommendation is made.

The Classical Impedance Curves were generated in order to provide guidance in understanding the Impact Impedance Curves (IICs) which would be typically obtainable from experimental impact testing of cadavers.

DIAGRAM OF SYSTEM	MATHEMATIC FORMULAS: IMPEDANCE Z – EQ.(10.7) MOBILITY $\mathcal{M}$ – EQ.(10.9)	IMPEDANCE IN THE COMPLEX PLANE	MOBILITY IN THE COMPLEX PLANE	MAGNITUDE OF IMPEDANCE	MAGNITUDE OF MOBILITY	IMPEDANCE ANGLE θ FIG.10.34
I.	$Z = c$ $\mathcal{M} = 1/c$					
2.	$Z = \dfrac{k}{j\omega}$ $\mathcal{M} = \dfrac{j\omega}{k}$					
3.	$Z = j\omega m$ $\mathcal{M} = \dfrac{1}{j\omega m}$					

SOURCE: Harris and Crede's *Shock and Vibration Handbook.*

FIGURE 1. Impedances and mobilities.
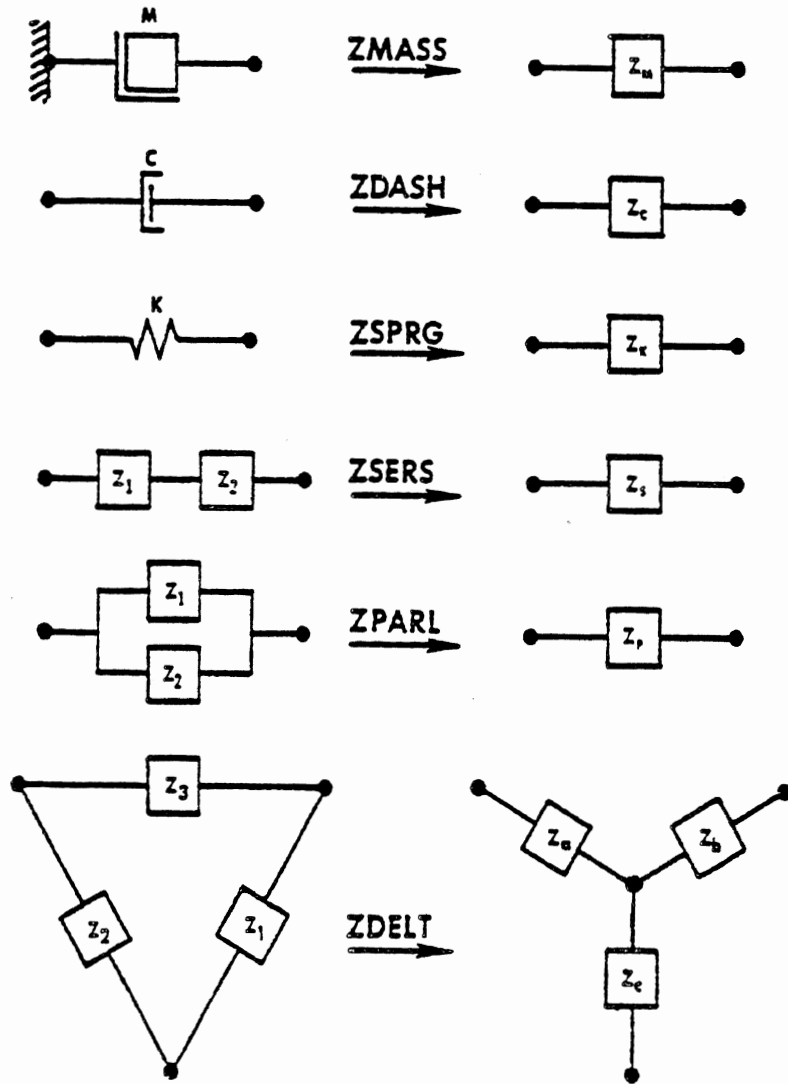
FIGURE 2. Basic impedance transformation.
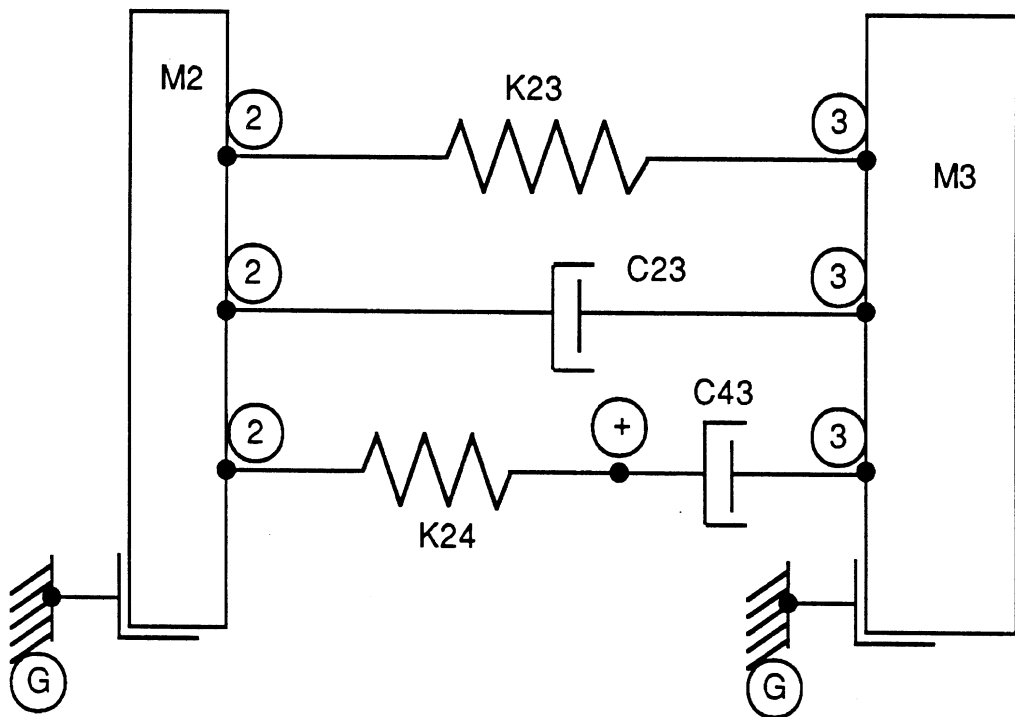
FIGURE 3. Lobdell lumped–parameter chest model.
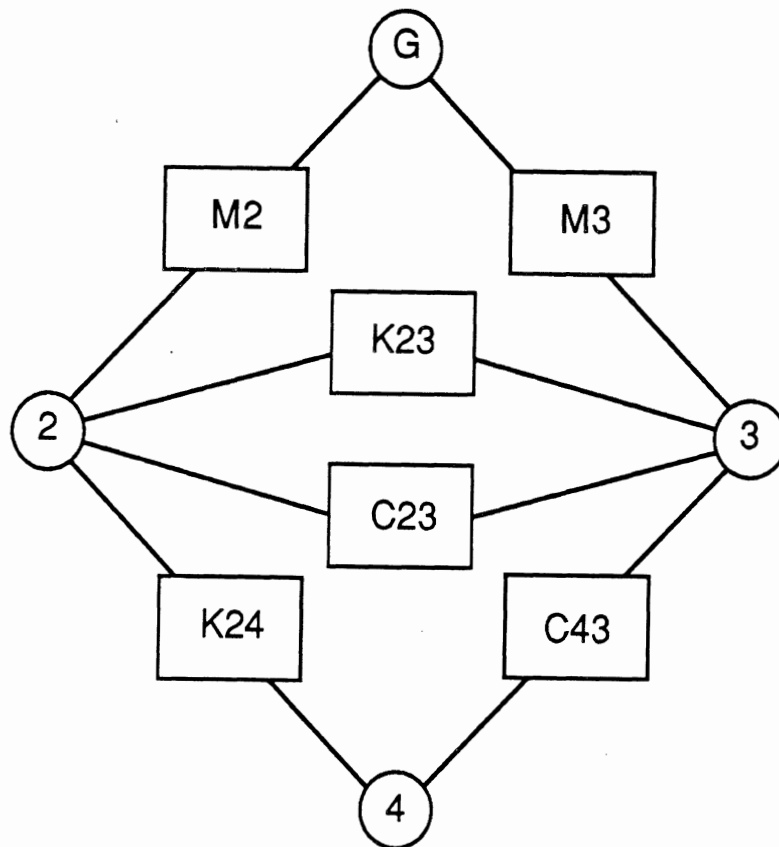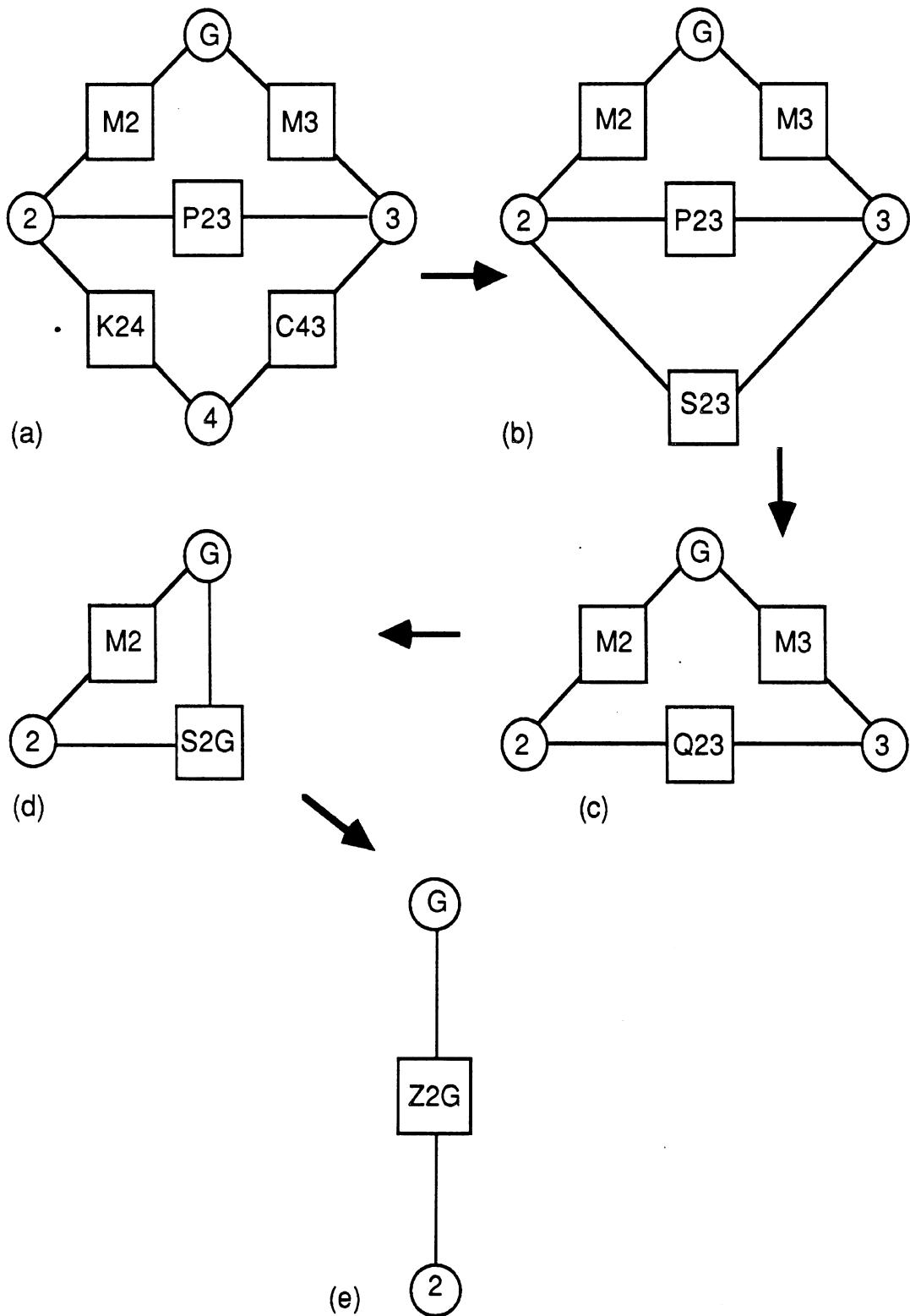
FIGURE 4. Network representation of Lobdell model.

FIGURE 5. Network reduction of Lobdell linear model.

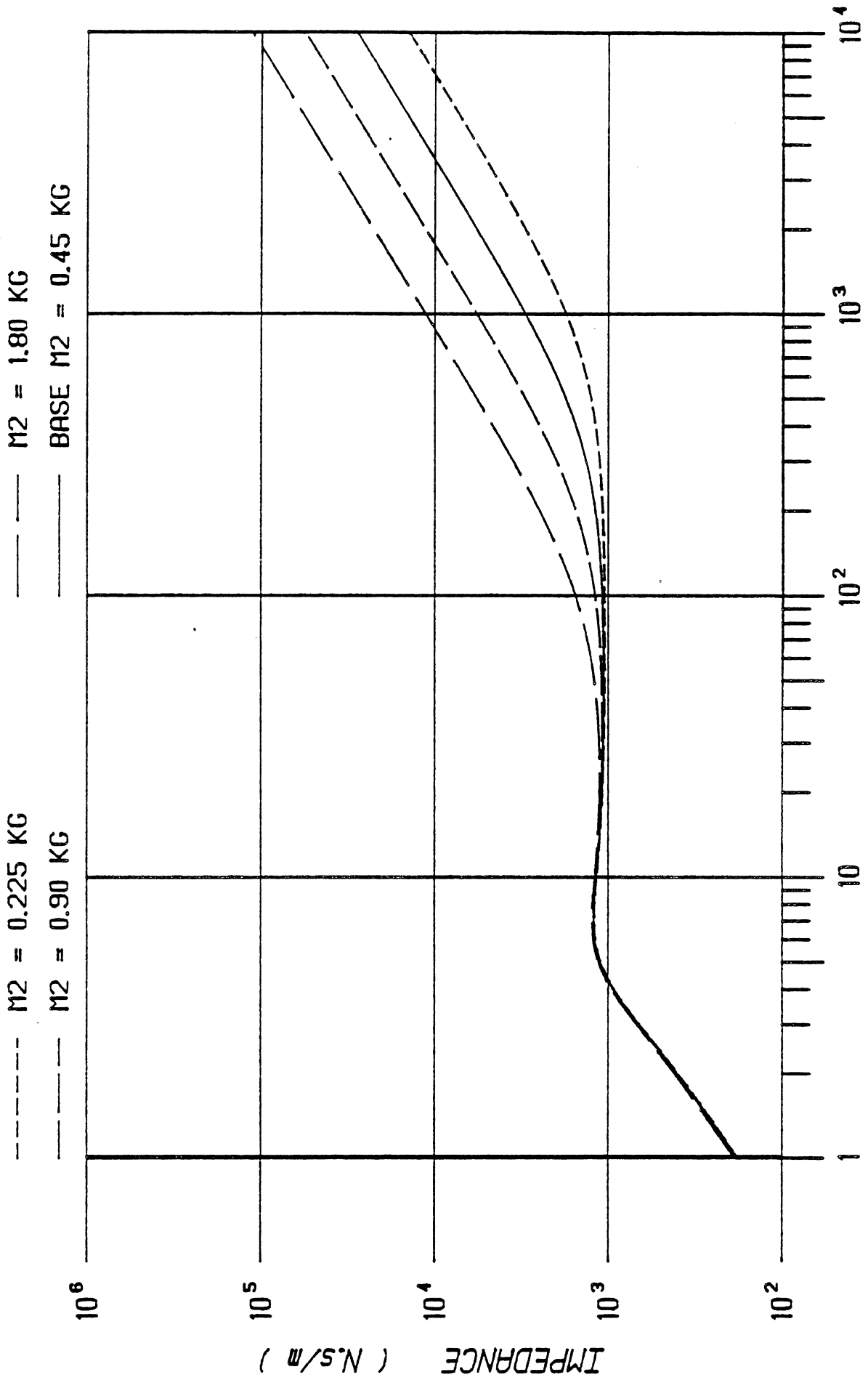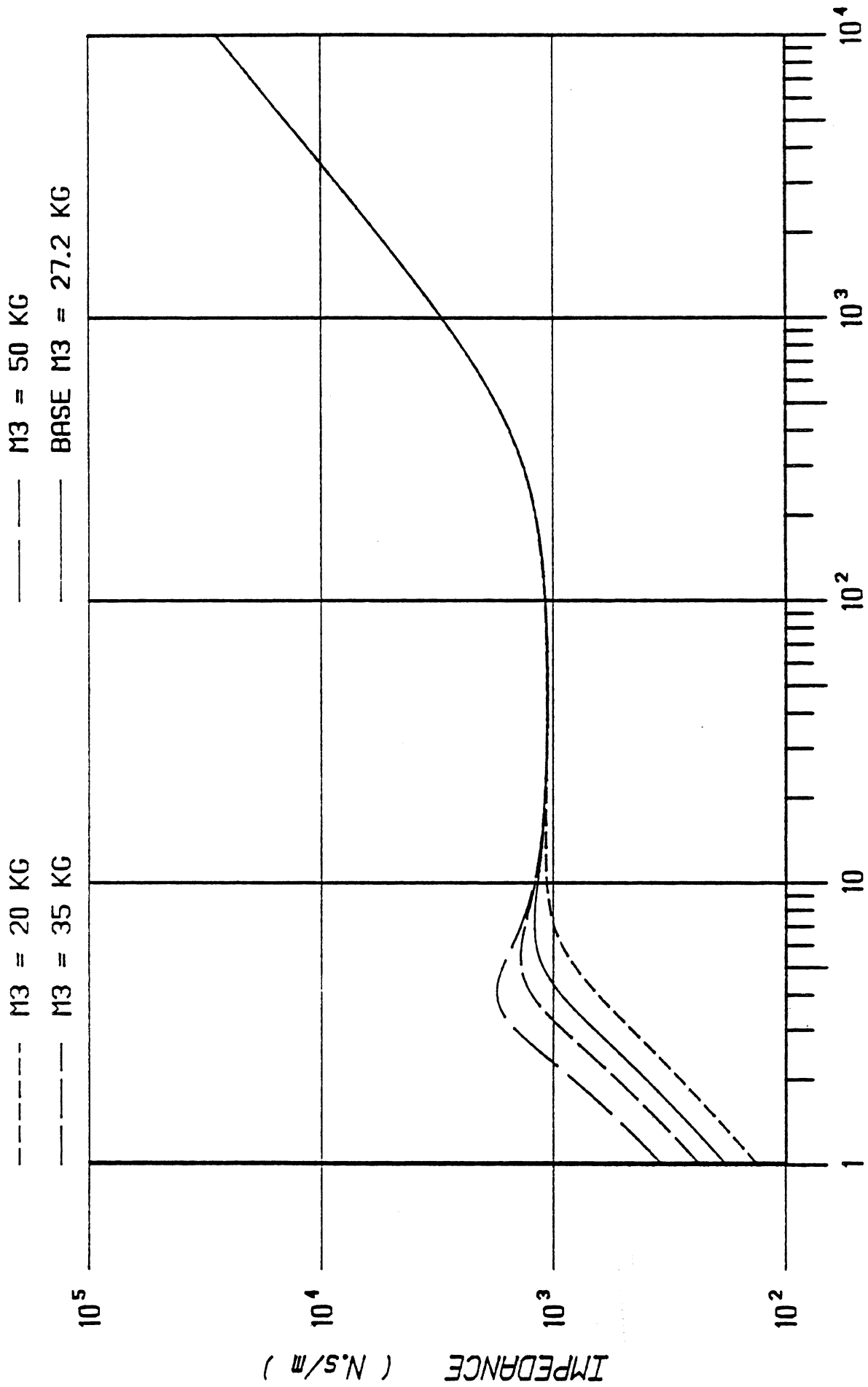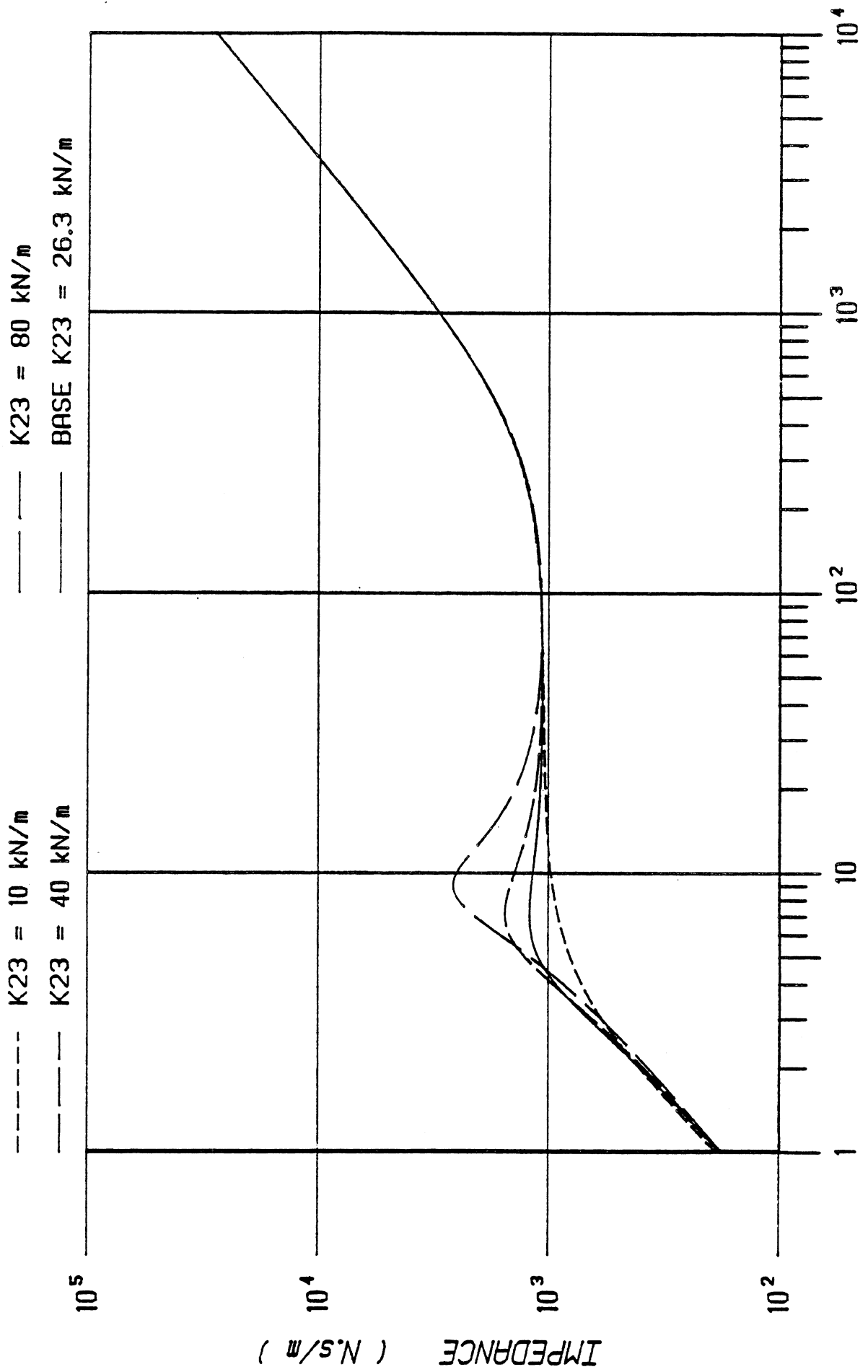FIGURE 6. Lobdell model: Effects of sternal mass M2.

FIGURE 7. Lobdell model: Effects of chest mass M3.
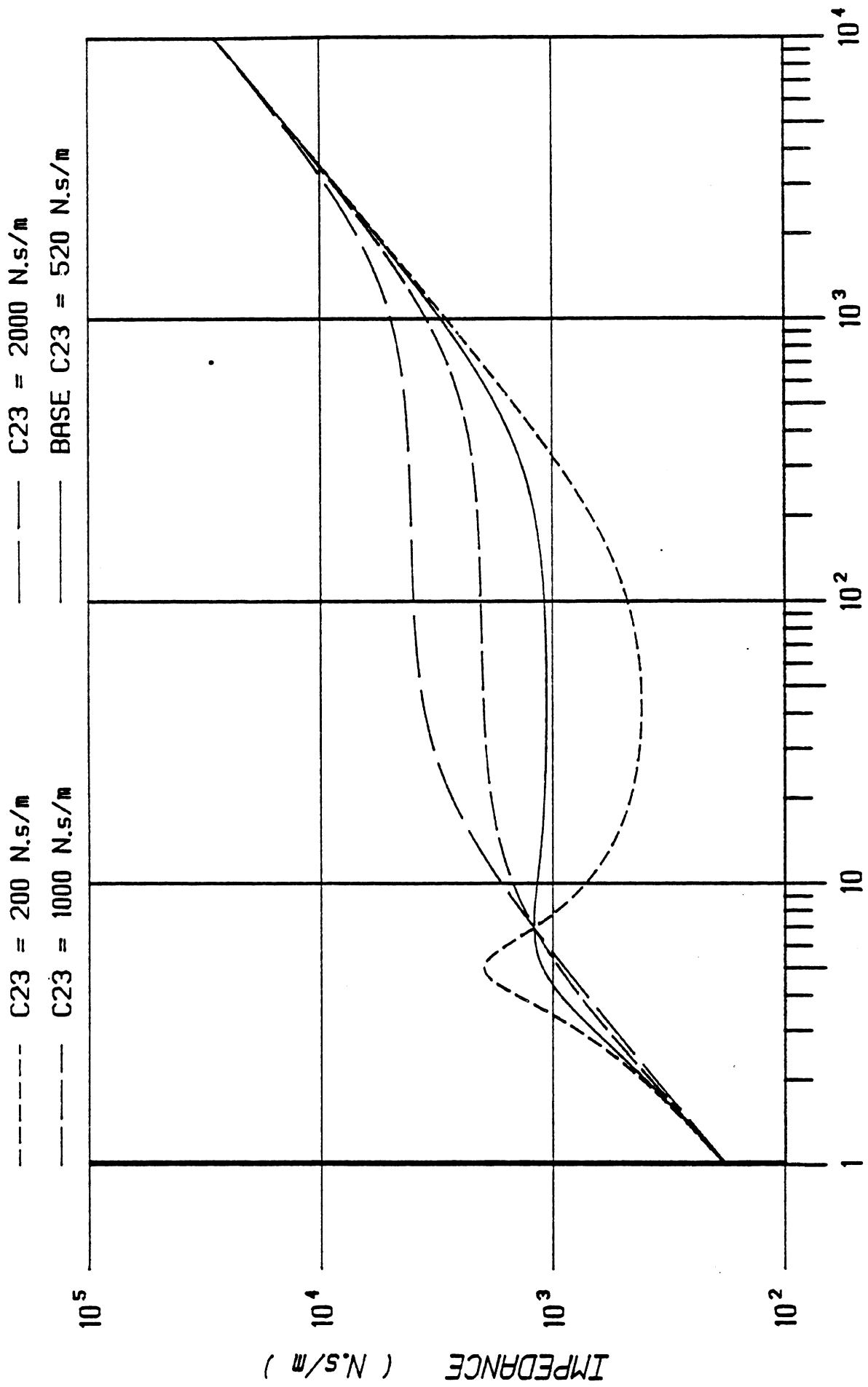
FIGURE 8. Lobdell model: Effects of chest stiffness K23.

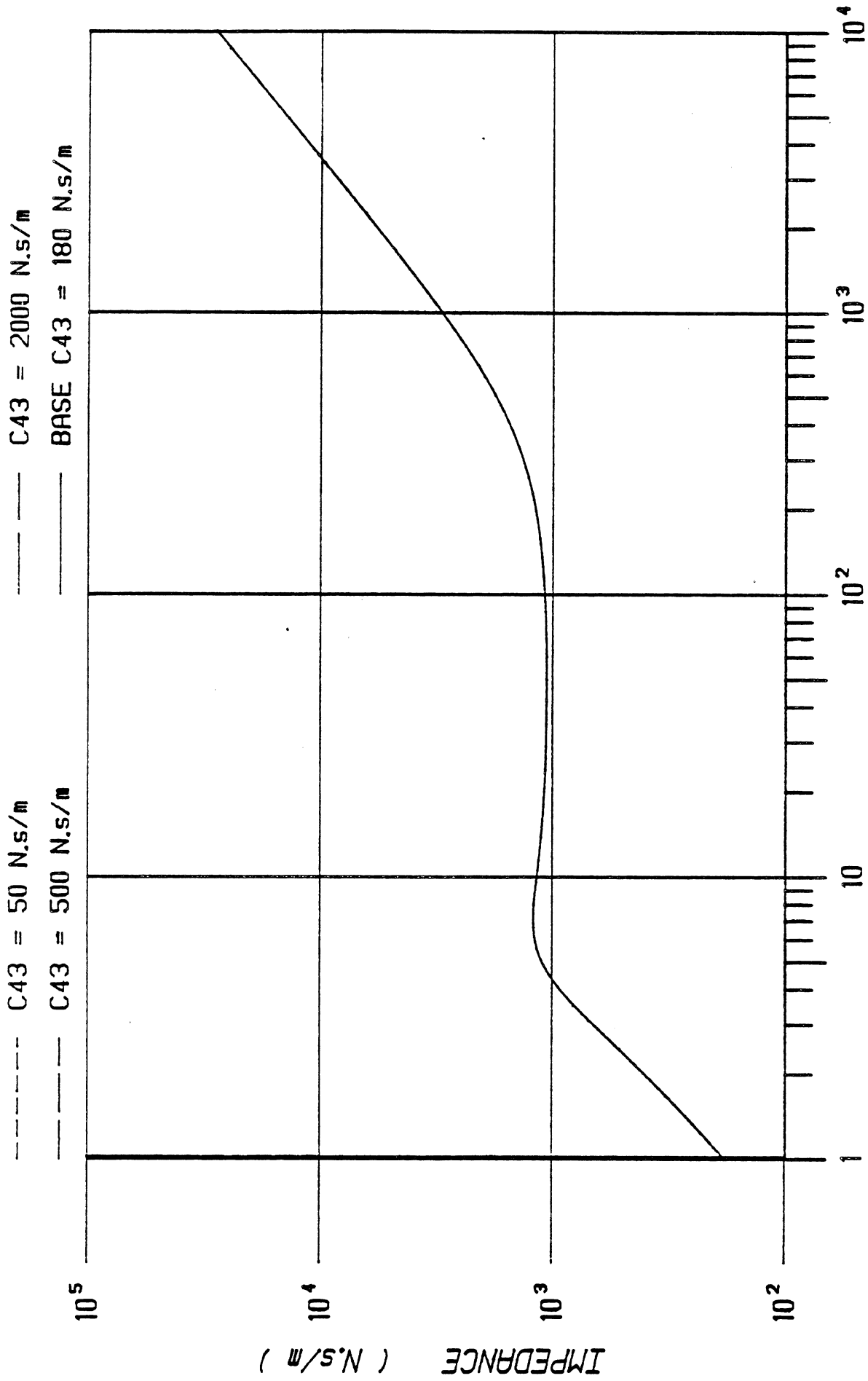FIGURE 9. Lobdell model: Effects of chest damping C23.

17

FIGURE 10. Lobdell model: Effects of viscoelastic damping C43.

18
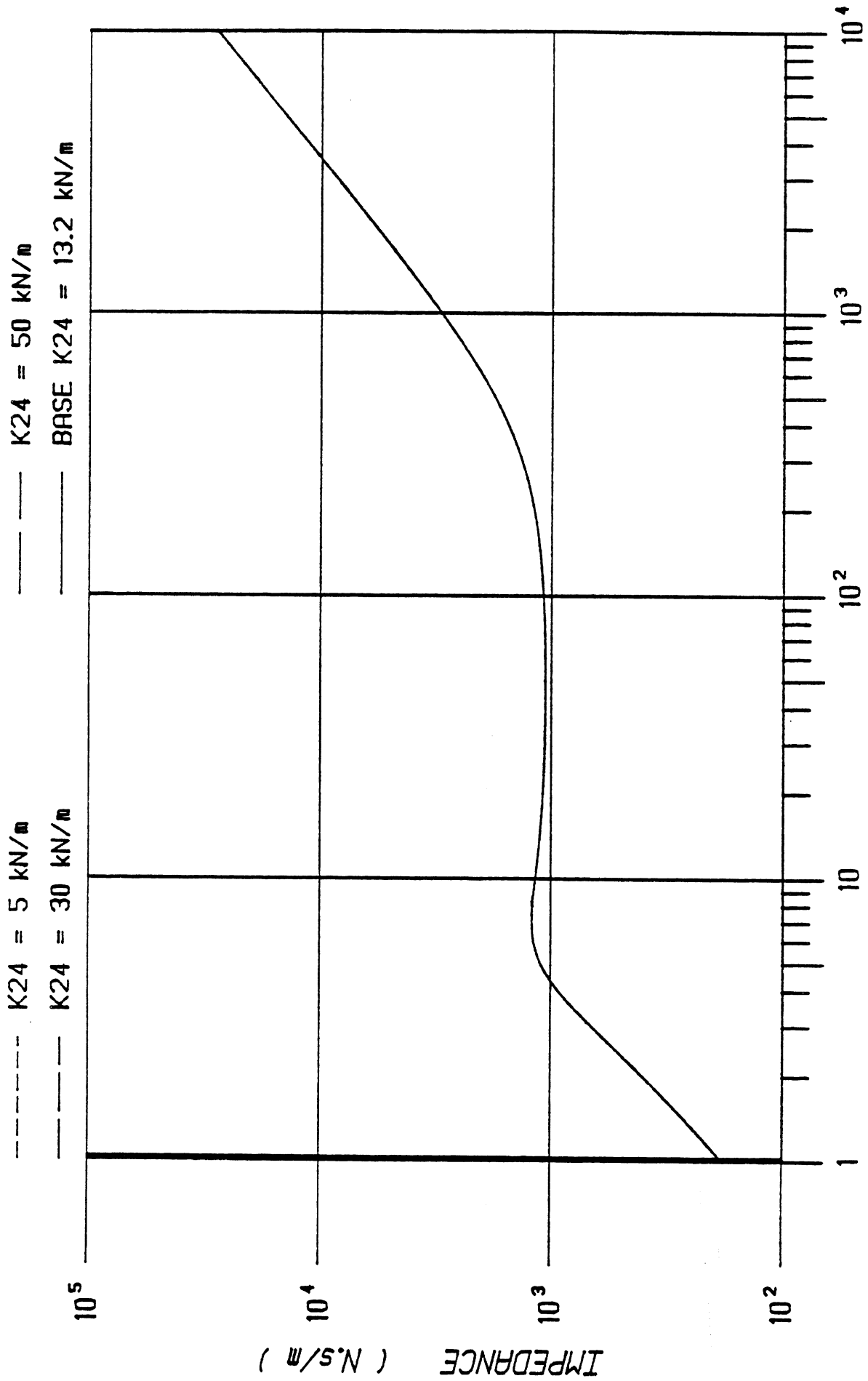
FIGURE 11. Lobdell model: Effects of viscoelastic stiffness K24.

IMPACT IMPEDANCE CURVES

Mechanical impedances of physical systems are experimentally obtained by applying sinusoidal excitation force to the system and measuring the steady-state acceleration response of the system. When all transients have died down, both excitation force and response would be at the same vibration frequency. When the system is linear (i.e., consisting of any network of simple masses, spring, and dampers), the response would also be sinusoidal.

Classically, mechanical impedance has been defined as the ratio of the peak force divided by the peak velocity. This ratio will be a function of the frequency of oscillation, and this function can be determined either analytically, when the system is simple, or measured experimentally, by repeating the forced vibration at selected frequencies.

In biomechanics impact testing, the luxury of steady-state forced vibration cannot (and usually is not) practiced for a number of reasons which will not be discussed in this report. However, all is not lost when the measured data is limited to a one-shot record of an "input" force and an "output" acceleration.

DEFINITION AND COMPUTATION OF THE IIC

At UMTRI, a method was developed and used with some success to obtain an Impact Impedance Curve from an impact force and an acceleration response. The IIC is based on two basic assumptions, one of which is mathematically correct, while the other has been shown to hold for most signals. These two assumptions are briefly discussed below.

The first assumption is derived from Fourier analysis and states that any random signal is the linear combination of sinusoidal components. Thus, both force and acceleration signals may be broken into their Fourier components and, when both signals are of the same length and at the same sampling rate, their respective components are defined at the same frequency points which range from the fundamental frequency up to the Nyquist rate. The impedance at each frequency point is the ratio of the Fourier coefficients of the force over those of the velocity, where the Fourier coefficient of the velocity is equal to the acceleration coefficient divided by the frequency, a simple integration in the frequency domain.

The second assumption deals with the problem of steady-state conditions and the initial conditions of the system. Recall that CICs are obtained from steady-state forced vibration of the system after all transients have died down. In impact testing, the whole signal available for analysis is a transient in itself. The issue of steady-state conditions can be resolved by accepting the first assumption that what looks like a transient is nothing but a linear superposition of steady-state responses at frequencies which are multiples of the fundamental. However, the initial conditions of "rest" cannot be easily removed from the above analysis since there must be a "transient" corresponding to each of the Fourier "steady-state" component.

In any case, there is nothing to prevent the definition of a new type of impedance curve, the Impact Impedance Curve (IIC), which is defined similarly to the CIC, except

21

that now the "peak" force and "peak" velocity are not obtained from classical steady-state forced vibrations, but are defined, instead, as the Fourier components of transient signals generated during a one-shot impact.

Computation of the IIC is straightforward. Given two digitized signals (force and acceleration), the Digital Fourier Transformation is applied to both using FFT routines. A typical FFT routine replaces the real signals of N points with its complex transform at N/2 frequencies. At each frequency, the complex impedance is defined as the product of the frequency times the ratio of the complex force over the complex acceleration. Finally, the magnitude and phase angles are extracted from the complex impedance and plotted against the frequency axis, starting with the fundamental.

ICCs OF FOUR ACTUAL IMPACTS

Four thoracic tests were selected from previous UMTRI pendulum tests. These were 77T053, 77T056, 78T059, and 78T062. The first three tests were frontal impacts, while the fourth was a left-side impact.

The first three curves (Figures 12, 13, and 14) were obtained using a previously developed UMTRI impedance program, designed for 100-msec signals sampled at 6400 Hz. These were IICs between the impact point where impact force is measured, and the RUR, RLR, and LLR* locations on the thorax. All three show an approximately constant impedance of about 1000 N·s/m between 10 and 50 Hz, indicating a dashpot-like behavior in this region; all three generally exhibited a dip between 60-70 Hz, indicating a resonance; and all three CICs exhibited a mass-like behavior beyond 100 Hz.

Since it was known that the Lobdell model has a resonance at about 7 Hz and a mass-like behavior below this resonant frequency, it was not possible to compute actual CICs below the fundamental of 10 Hz (1/0.100 sec). However, the general constant behavior of the CICs agreed with the behavior of the Lobdell model as determined from its CICs, at least in the 10- to 50-Hz range.

A new impedance program was written and used to plot the IICs over a wider frequency range. Since the sampling was fixed at 6400 Hz for all four tests, the highest frequency that could be observed would still be limited to the Nyquist frequency of 3200 Hz. However, by extending the signal from 640 points to 8192 points (by zero-filling the extension), the fundamental is lowered to below 1 Hz.

Using the new impedance program, the IICs of six thoracic transducers (LUR, LLR, RUR, RLR, UST, LST) from four thorax impact tests (76T053, 76T056, 76T059, 76T062) were generated. Figures 15 through 20 are overplots of all four tests for each of the six transducers. Figures 21 through 24 are IIC overplots of all rib transducers for each of the four tests. Figure 25 through 28 are overplots of the two sternal transducers for each of the four tests. From these plots of Impact Impedance Curves, some of the observations that may be made are discussed briefly below.

---

*RUR=right upper rib, RLR=right lower rib, LLR=left lower rib, LUR=left upper rib, UST=upper sternum, LST=lower sternum.

1. All twenty-four IICs are noisy because of the nature of the computation process, the limitation of the sampling rate and record length, and because of the bandlimiting of the frequency contents in the recorded signals. However, overplots (and perhaps corridors) seem to bring out general characteristic features which would not be otherwise obvious from a single IIC.

2. The impact point IICs exhibit a constant mass behavior up to about 50 Hz, and not up to 10 Hz as postulated in the Lobdell model. The frontal impact tests exhibit a value in the range of 20 kg (Figure 20, lower sternal accelerations), while the one lateral test exhibits a corresponding value of about 30 kg (Figure 15, left upper rib accelerations). These values represent effective masses of 23% and 60% of total body weight, respectively.

3. The sternal IICs for all tests appear to be flat in the 10-100 Hz region, in agreement with the CIC of the Lobdell model.

4. It appears that a natural frequency near the 100 Hz is a characteristic of all the IICs. This is more obvious in some curves than in others. However, no natural frequency is obvious at or near the 7 Hz frequency as postulated in the Lobdell model. This could be a limitation of the computation process which artificially extends the signal to obtain IIC points below the original fundamental.

5. The IICs for the "remote" accelerometer locations (that is, RUR, LUR, RLR, and LLR for frontal impacts and UST, LST, RUR, RLR for lateral impact) exhibit similar plots. This indicates potential applicability of the IICs to global design criteria for the AATD thorax.

6. The sternal mass cannot be readily determined because it would show up as a mass-like trend near the high end of the frequency spectrum. However, the general behavior of the IICs between 100 and 1000 Hz seems to fall down to an anti-resonance in some transducers at about 500 Hz, or remain constant in this range. If this were a realistic behavior, then the sternal mass would appear as a mass-like trend beyond the 500 Hz. This is consistent with the Lobdell model behavior which indicates that the low mass-like trend generally starts well beyond 100 Hz.

7. Without the aid of a lumped-parameter model, it would only be a guess to "read off" a value for a spring constant along the sloping-down constant-K lines.

Interpretation of actual test IICs must be based on known impedance characteristics. Thus, one would postulate a model, produce its impedance curve, perhaps conduct some parametric study, and then compare the IICs to known model behavior. When the model is linear, Classical Impedance Curves are easily produced as shown in an earlier section of this report.

However, when the model is non-linear, CICs are meaningless, and one would generate impedance curves by exercising the model in forced-vibration mode (i.e., sinusoidal forcing function) at several frequency points, then compute an "impedance" as the ratio of the steady-state peak input force over peak response velocity. Furthermore, since Impact Impedance Curves are generated in an unconventional method, similar IICs for a known model should be generated in order to understand the effects of the Fourier computations.

ICCs FOR THE LOBDELL MODEL

In order to provide a guide in the interpretation of the Impact Impedance Curves from actual tests, the linear version of the Lobdell model was exercised. This required that segments of the program be rewritten (at WSU) to produce equally-spaced output response from the integration, and to extend the length of the output to over 1000 points.

The input to the model was constructed by taking a WSU sled pulse and modifying the magnitude and sampling interval to simulate a typical impact force from a pendulum or a cannon test. Initially, the impact force was bandlimited to 100 Hz, since we were interested in impedances in the 10-100 Hz range. This impact force and its spectrum are shown in Figures 29 and 30. Responses of the model at the sternal mass M2 and chest mass M3 are given in Figures 31 through 34 for four combinations of the K23 and C23 models. The IICs were then generated and are given in Figures 35 through 38.

It was immediately evident that by bandlimiting the impact force to 100 Hz, impedance curves became noisy beyond that point. This is understandable since by dividing two extremely small Fourier coefficients at the high frequencies, the result is subject to rounding and truncation errors, making the impedance "jump" up and down in an unpredictable fashion. However, several general observations may be made. The first is that the IIC appears to remain constant over the 10-100 Hz range when K23 and C23 are both linear, and that the high-frequency behavior is mass-like, similar to what a CIC would indicate.

The second observation is that the IIC exhibits a sudden drop near the 50-Hz frequency when the damping is bidirectional and for both linear and bilinear springs. This may be explained by the two different damping constants used to define the bidirectional damper. The last observation is that in Figure 38 (bilinear spring and linear damper), the low-frequency trend is clearly mass-like. Thus, although not definitive, these IICs indicated that some general conclusions may be drawn about the system's mechanical characteristics, but no accurate values could be extracted.

In an attempt to remove the suspected causes for crude and noisy CICs, three "unfiltered" pulses were generated and used to drive the Lobdell model in two different modes: a linear and bilinear K23 spring, while C23 was kept linear. Responses of the model were then used to generate the IICs shown in Figures 39 and 40.

Clearly, the retention of all frequencies available in the signal improves the noise level of the IIC in the high-frequency range. Furthermore, when the model is completely linear, the IIC appearance is identical to that of the CIC, within unavoidable rounding and computational errors. Thus, it may be concluded that, when there is control over the frequency content of the test signals (i.e., when there are sufficiently high frequencies), Classical Impedance Curves may be approximated by Impact Impedance Curves.

Since CICs are defined only for linear systems, the presence of non-linearity in the system prevents the generation of a CIC; however, IIC can still be generated and appears to provide important clues to the characteristics of such nonlinearity. This is evidenced by Figure 40 where three IICs were generated for the Lobdell model with a bilinear spring. The three IICs are consistent (again within computational error) and exhibit a trend distinctly different from a linear system's CIC. For this non-linear system, the impedance between 10 and 50 HZ appear to fall along a constant K-line, before it rises again along a constant mass line. This is reminiscent of a 2-mass spring, dashpot linear system (e.g., the MSC model), except this behavior is the result of non-linearity of the spring.

In summary, Impact Impedance Curves, when used in conjunction with lumped-parameter models, are useful for providing insight into the mechanical characteristics of a system and can provide estimates of the model parameters. The limitations on the frequency content as well as the duration of available test signals preclude the extraction of precise values for system parameters without the aid of modeling.
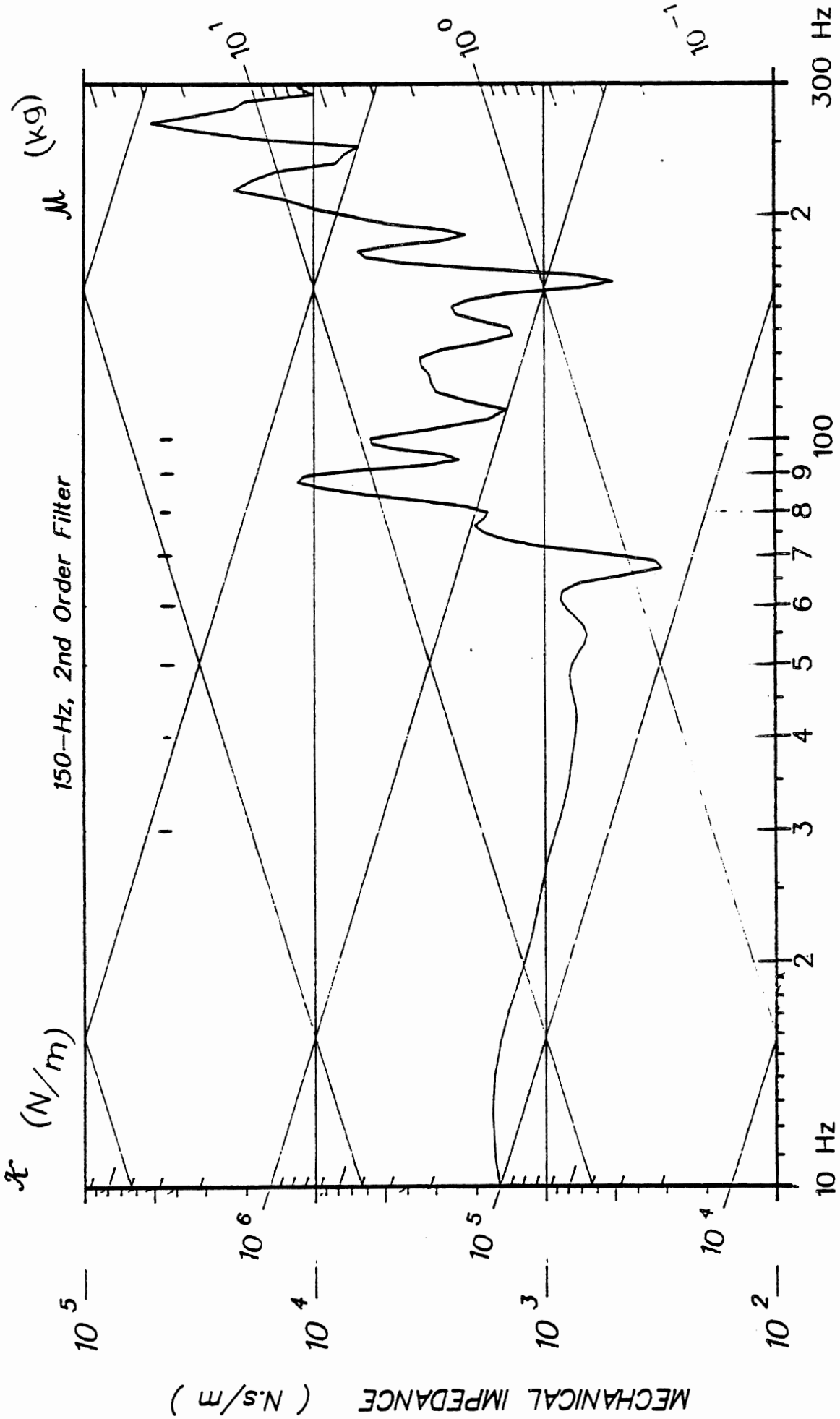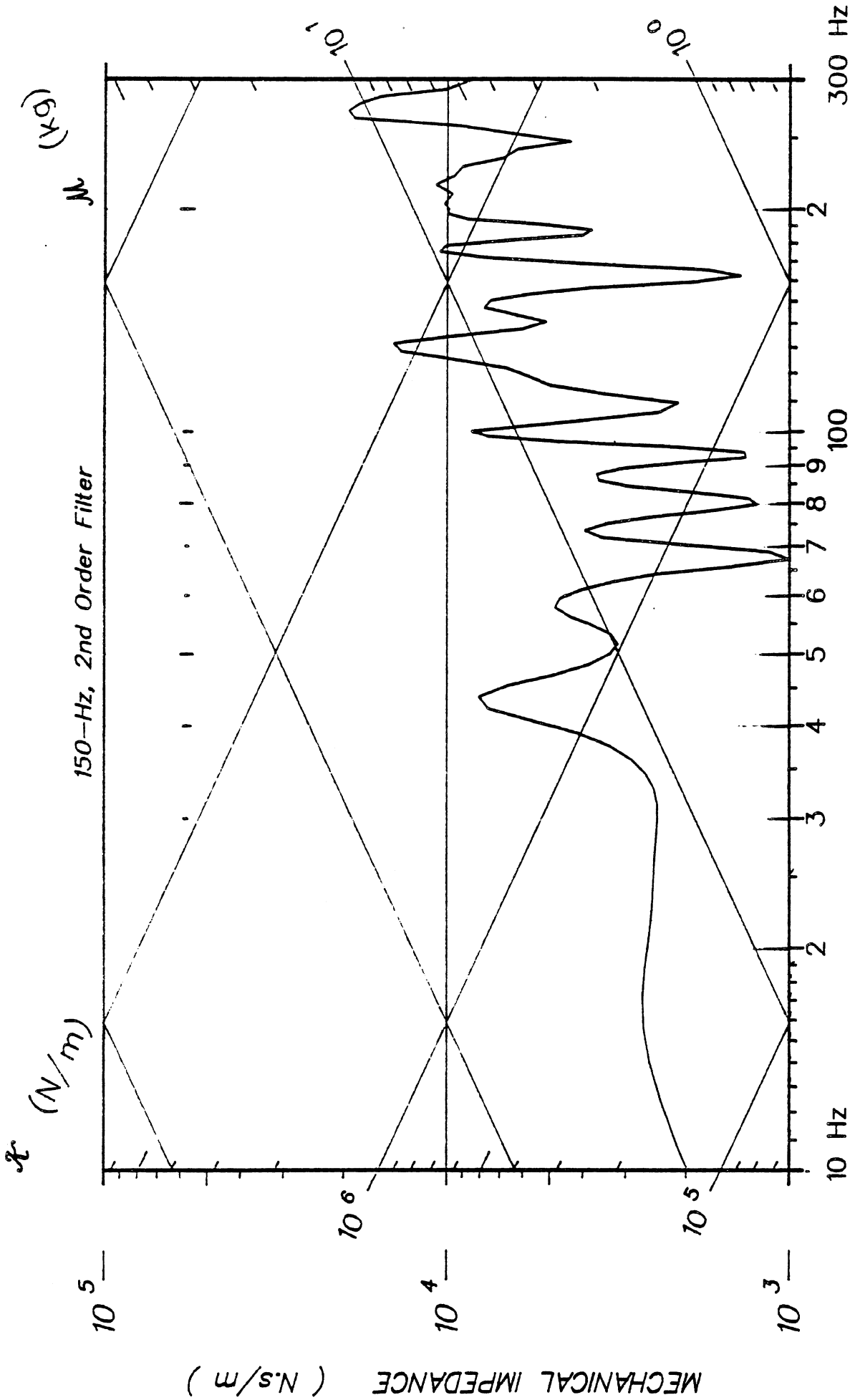
FIGURE 12. Mechanical impedance for RUR.

26
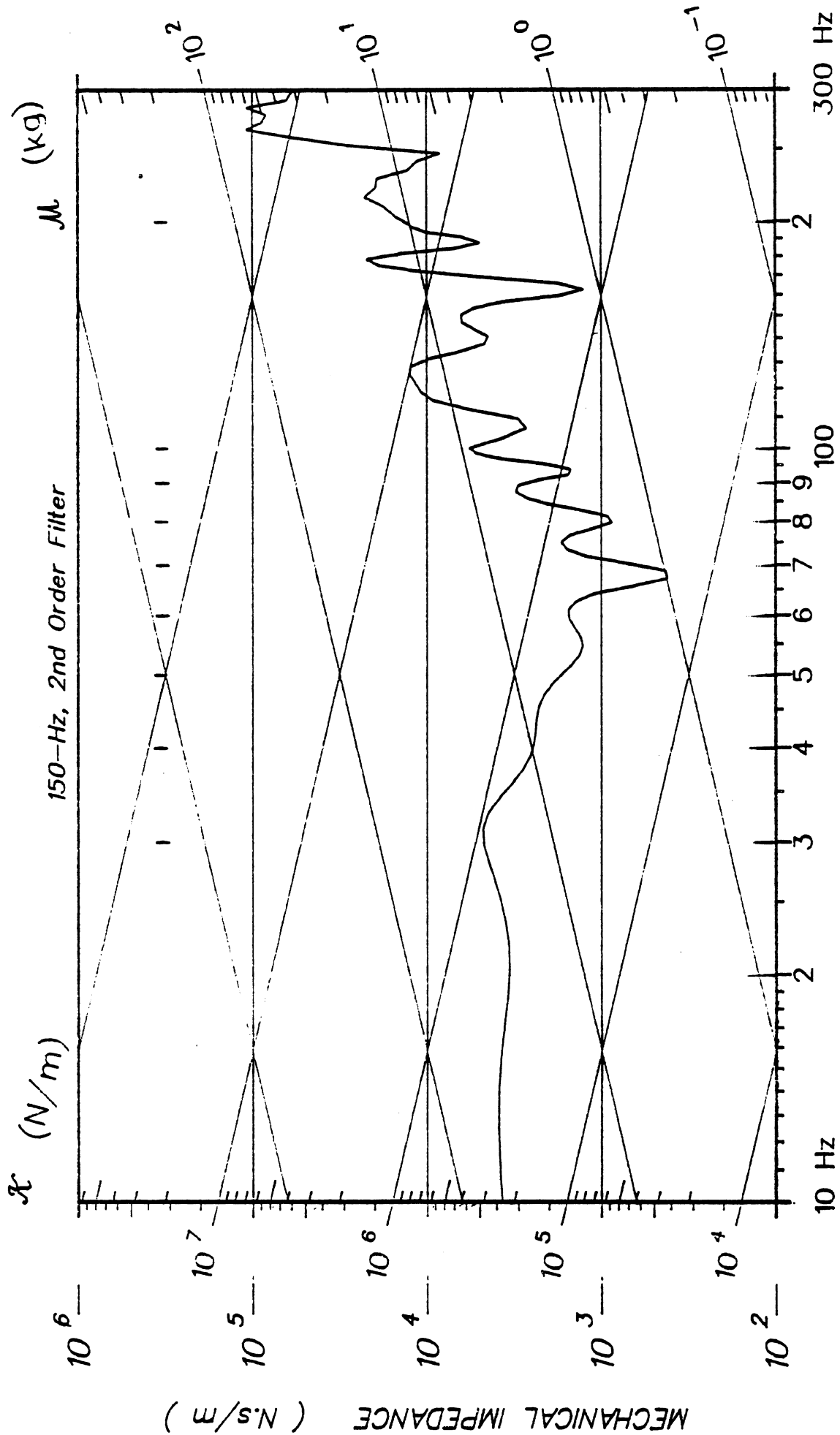
FIGURE 13. Mechanical impedance for RLR.

FIGURE 14. Mechanical impedance for LLR.

28
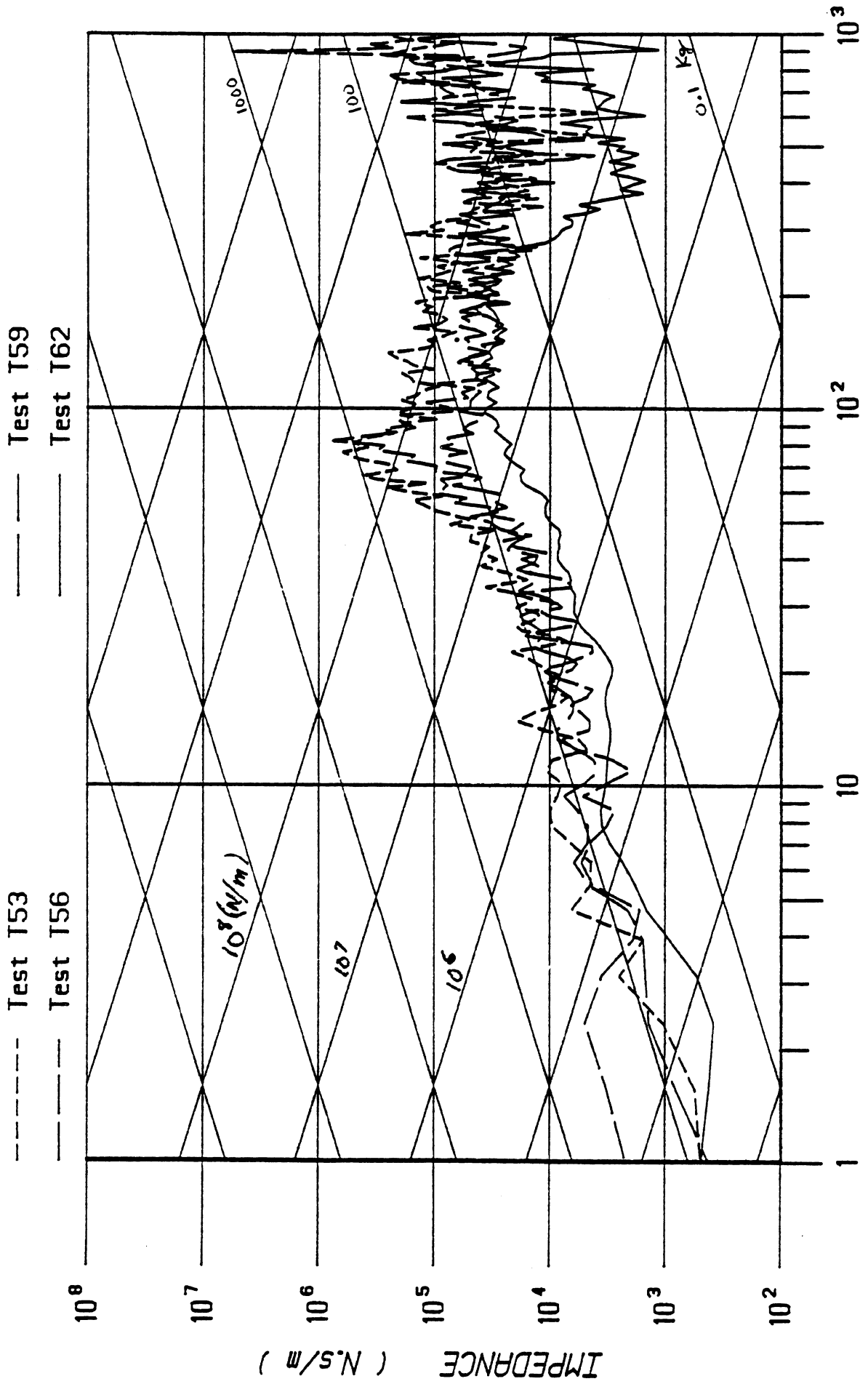
FIGURE 15. Impact impedance curves, location: LUR.
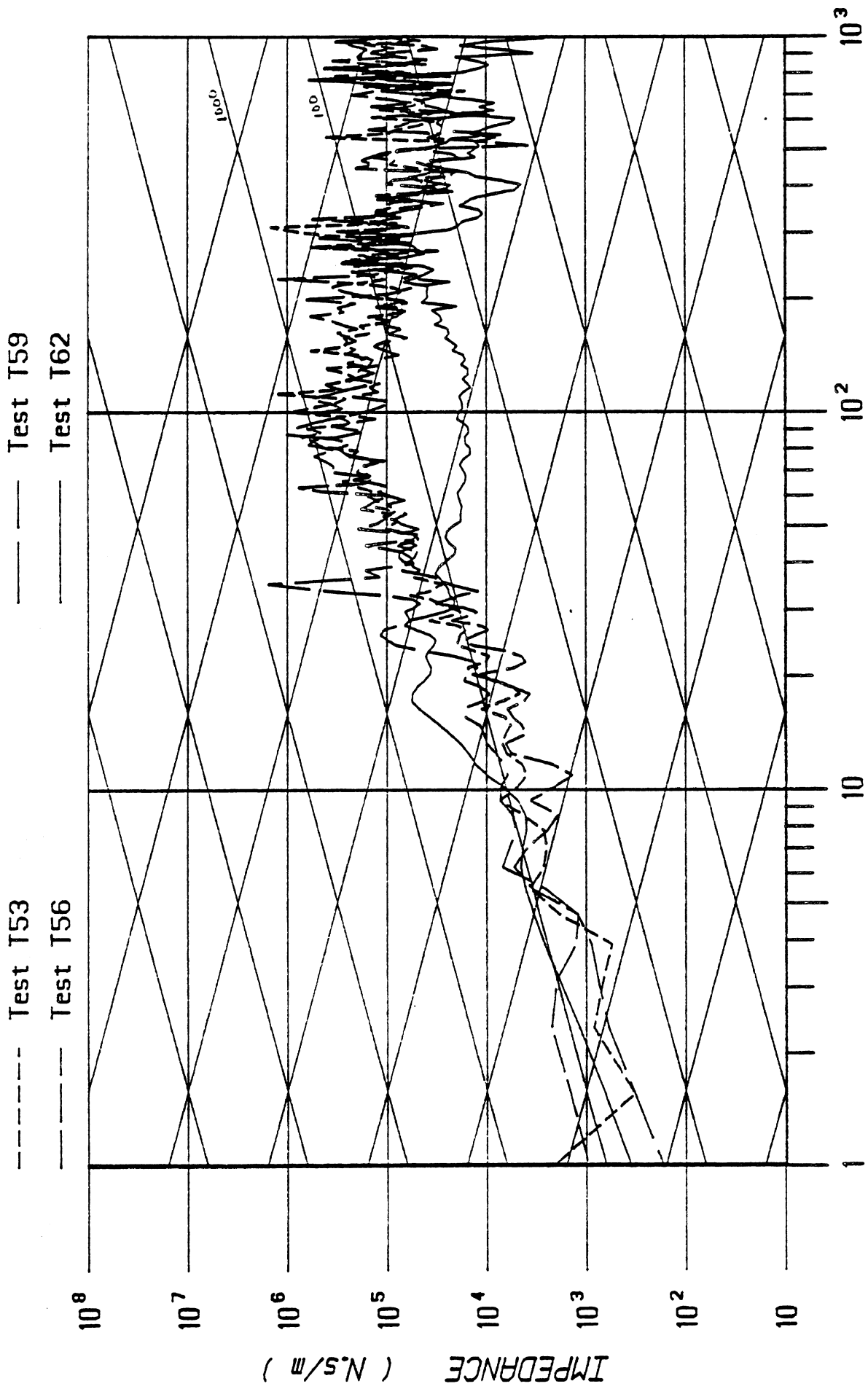
FIGURE 16. IICs at location LLR.
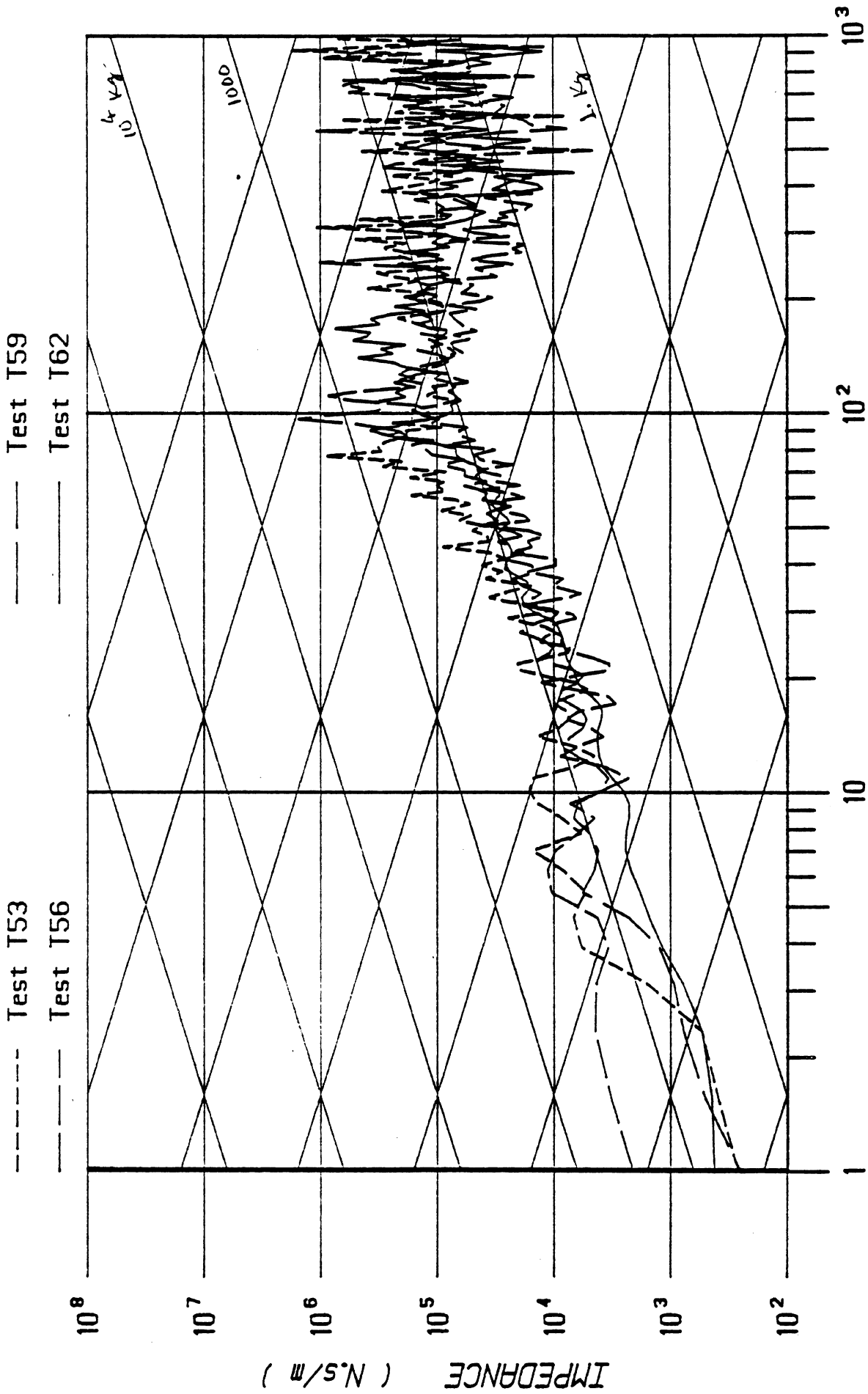
FIGURE 17. IICs at location RUR.

31
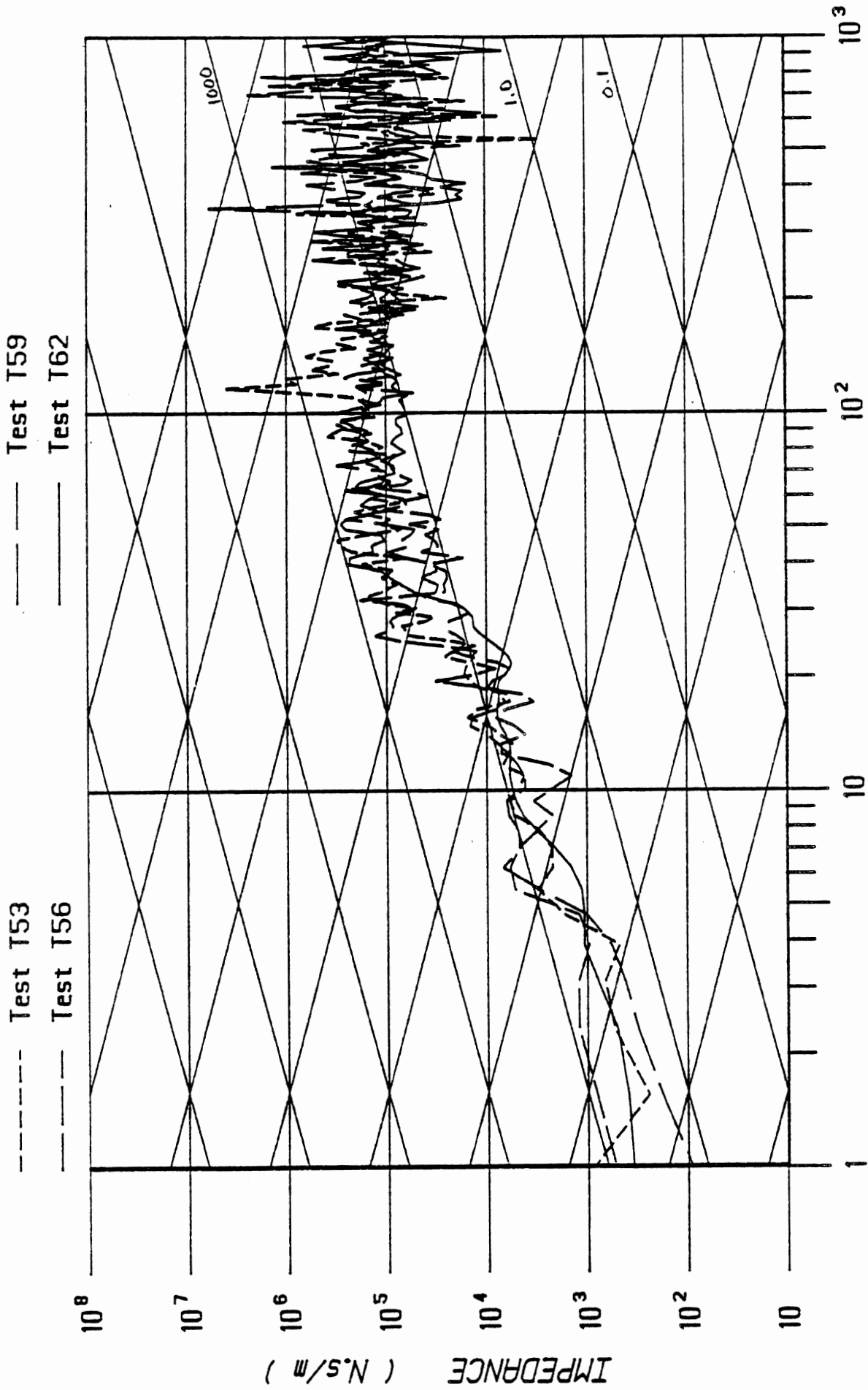
FIGURE 18. IICs at location RLR.
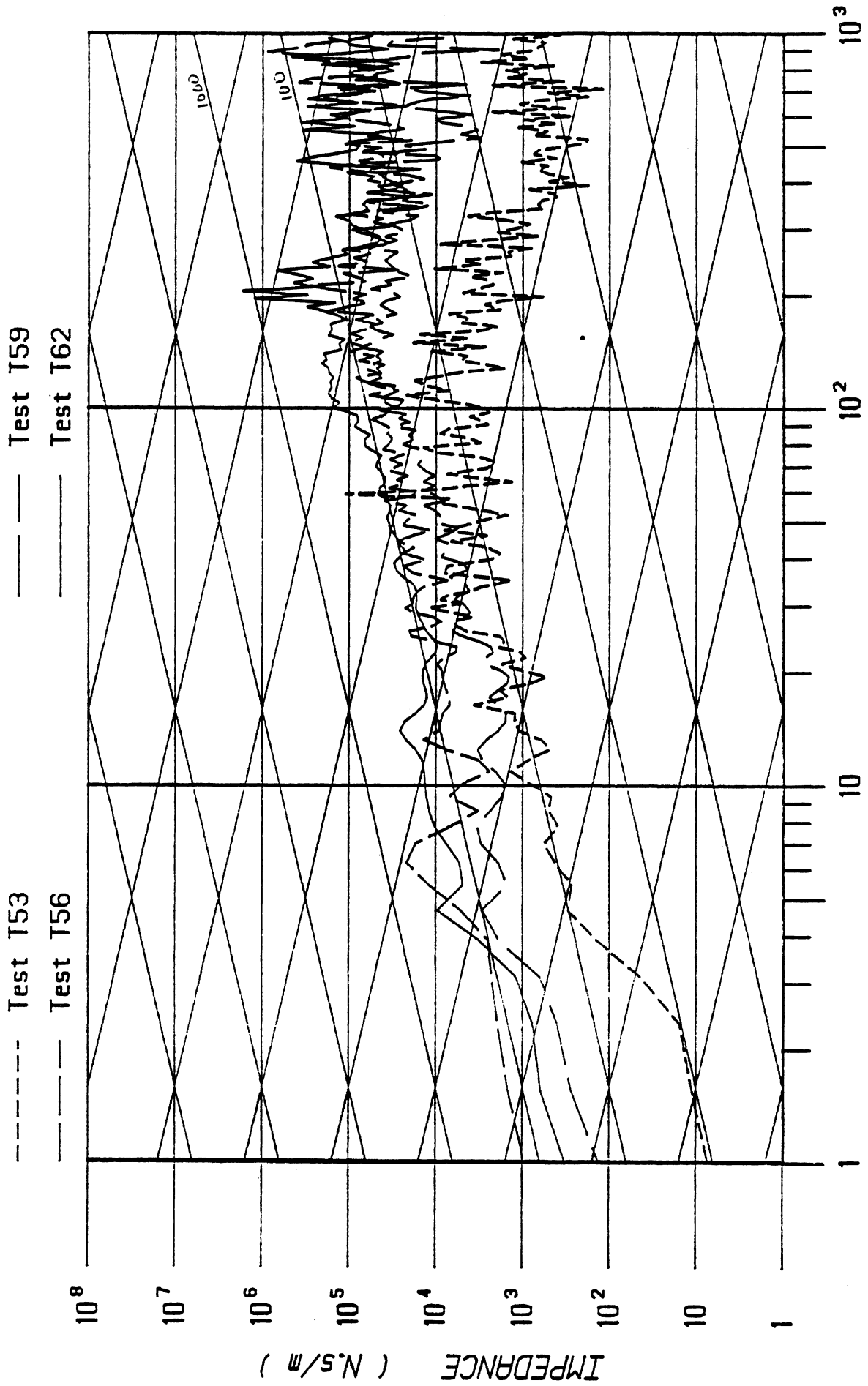
FIGURE 19. IICs at location UST.
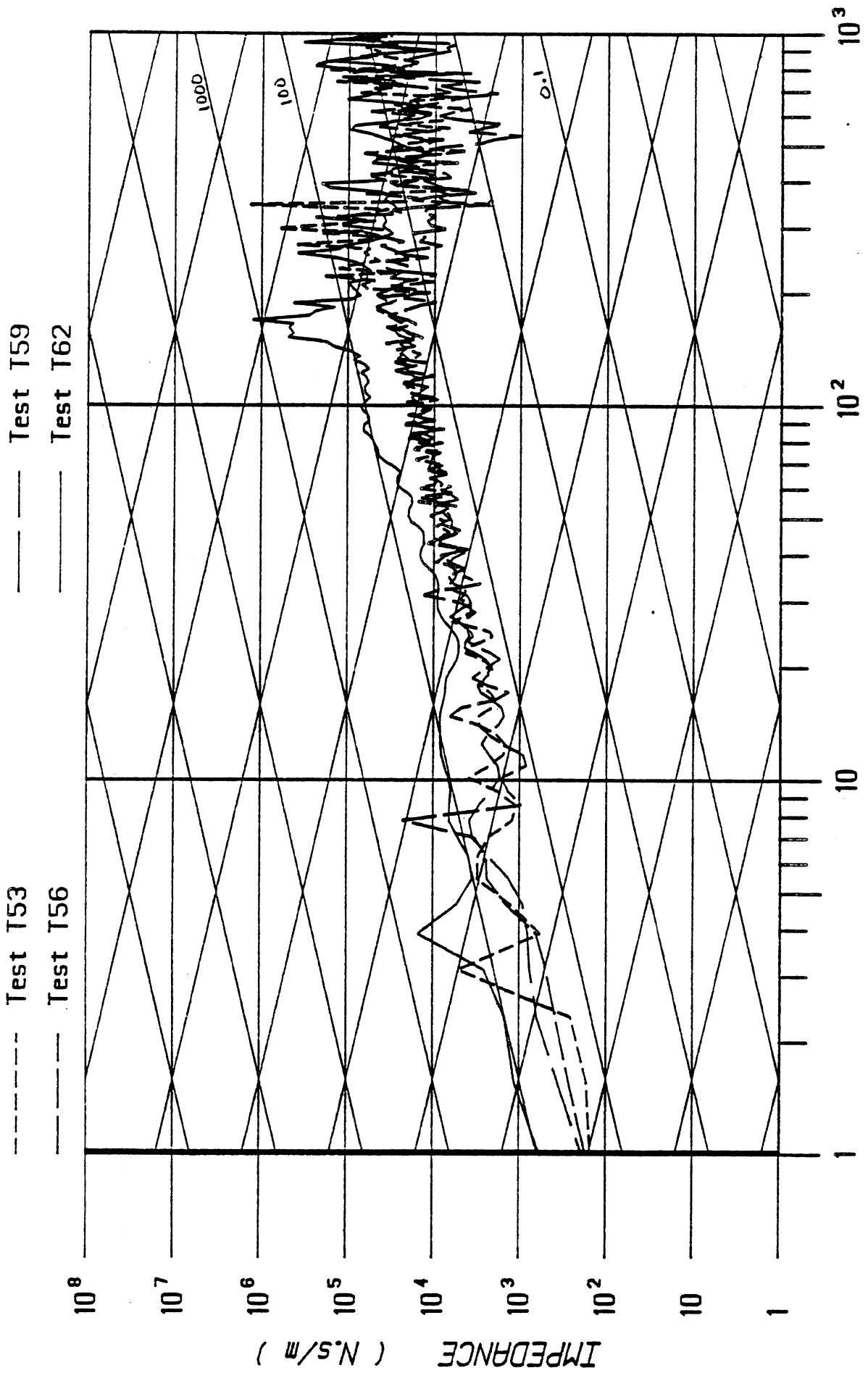
FIGURE 20. IICs at location LST.
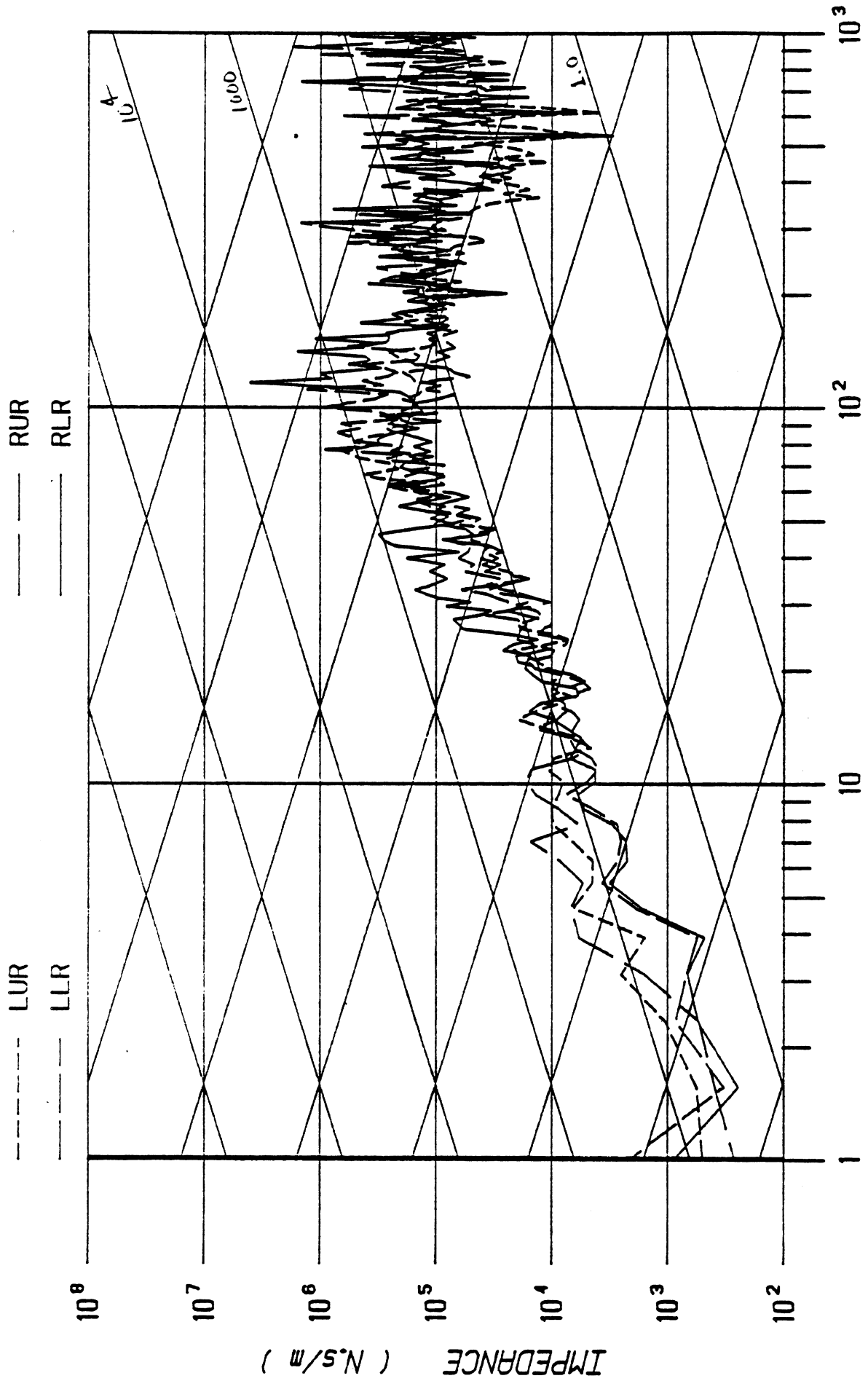
FIGURE 21. Impact impedance curves, Test T053.
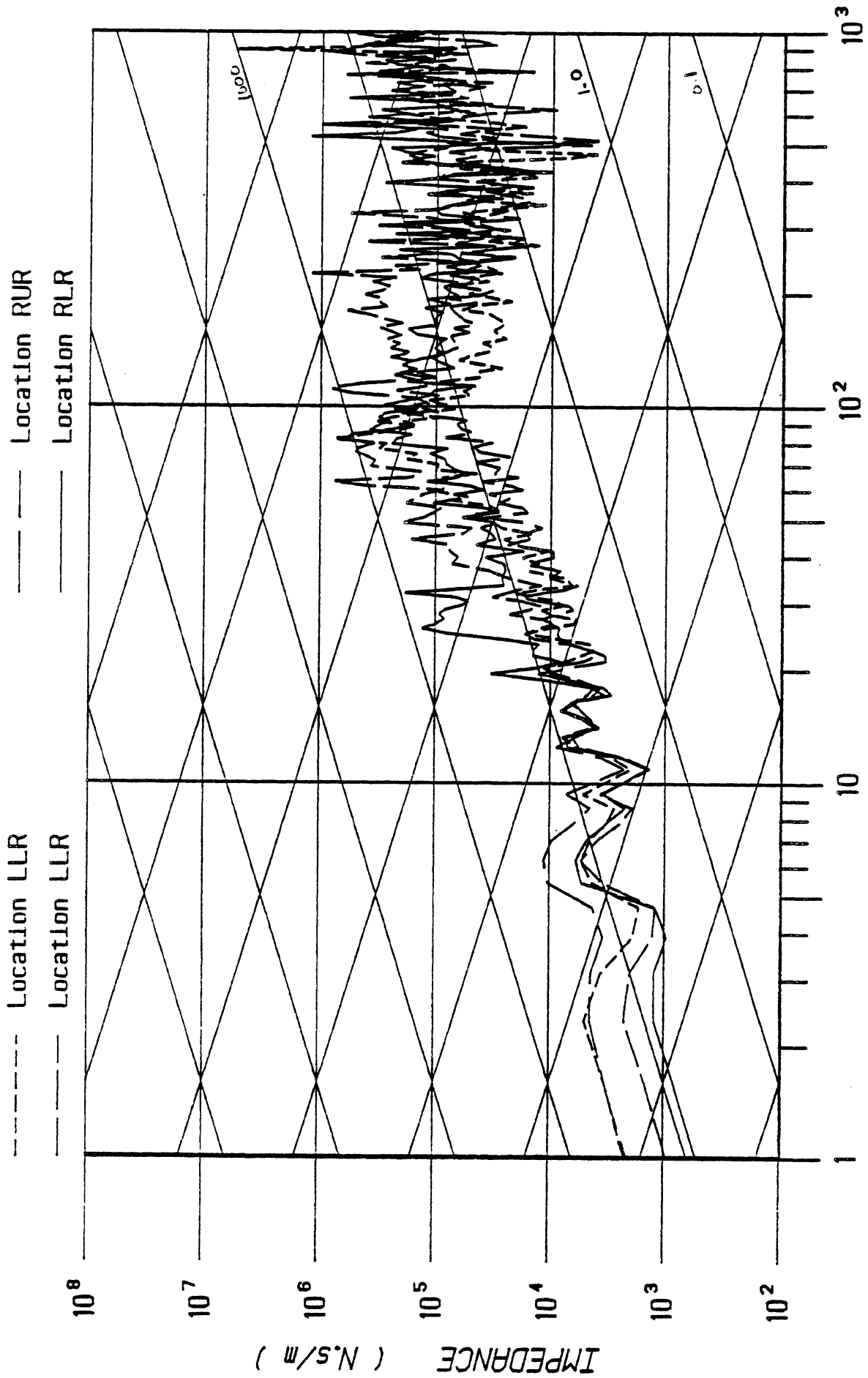
FIGURE 22. IICs for Test T056.

36
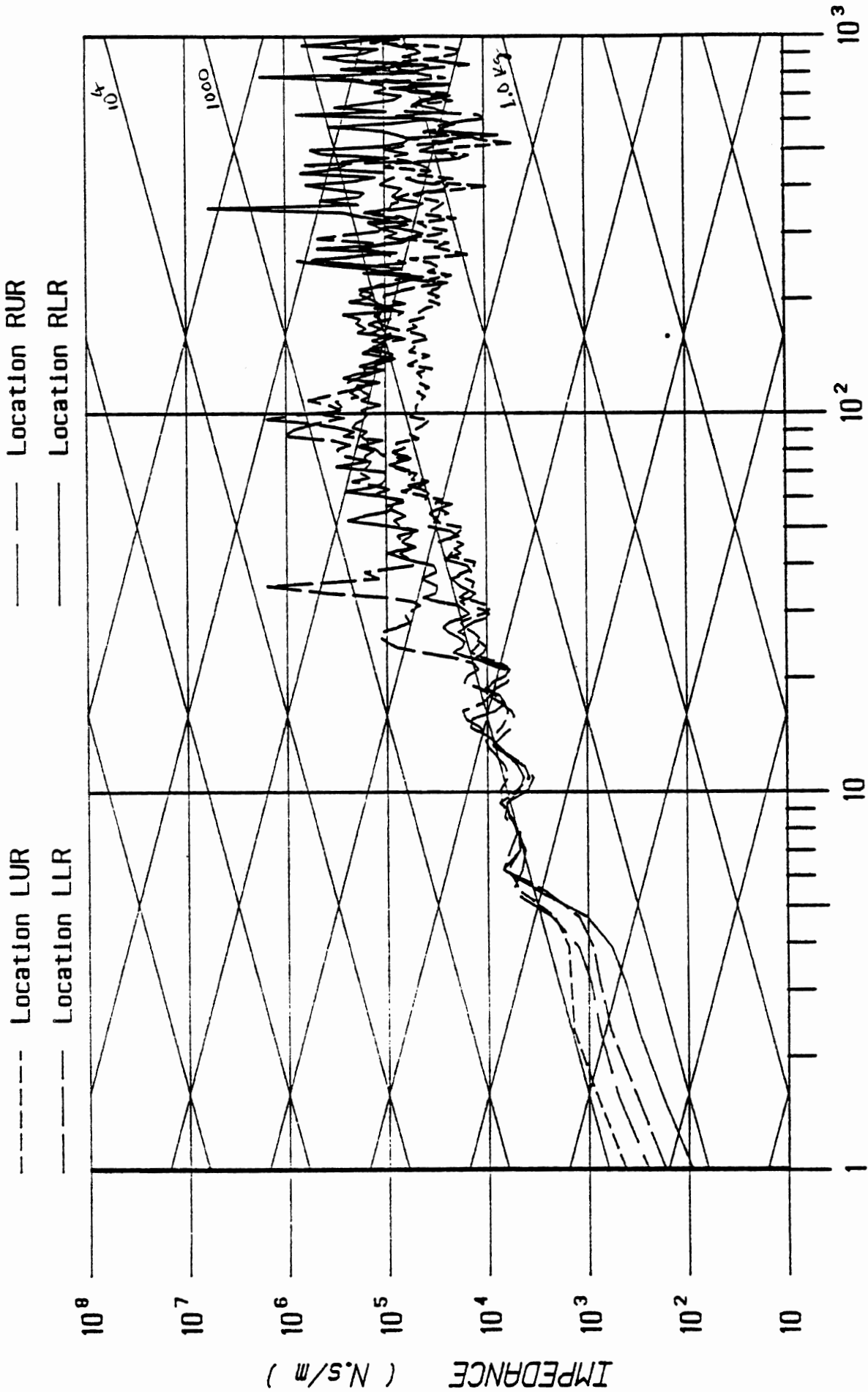
FIGURE 23. IICs for Test T059.

37
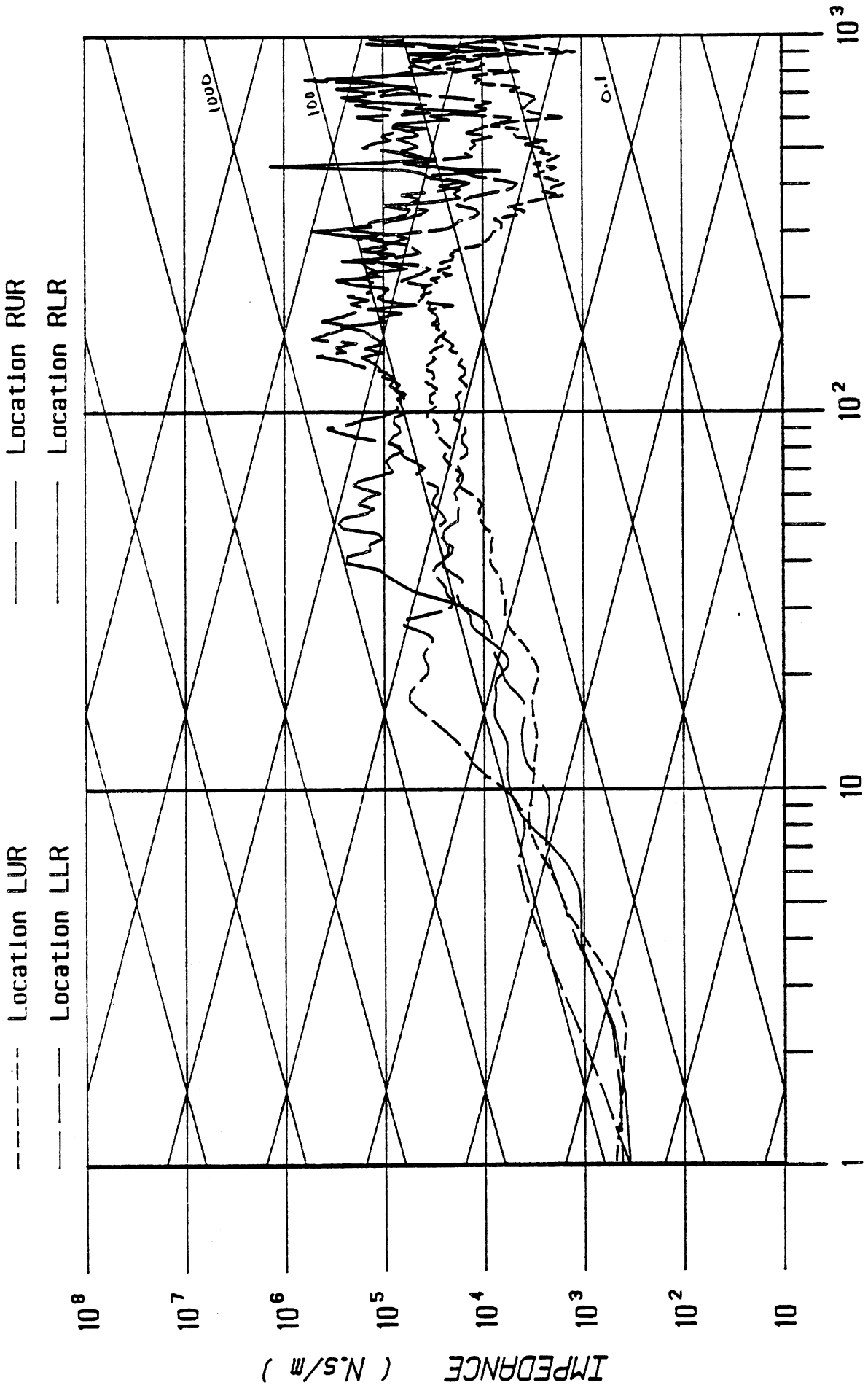
FIGURE 24. IICs for Test T062.
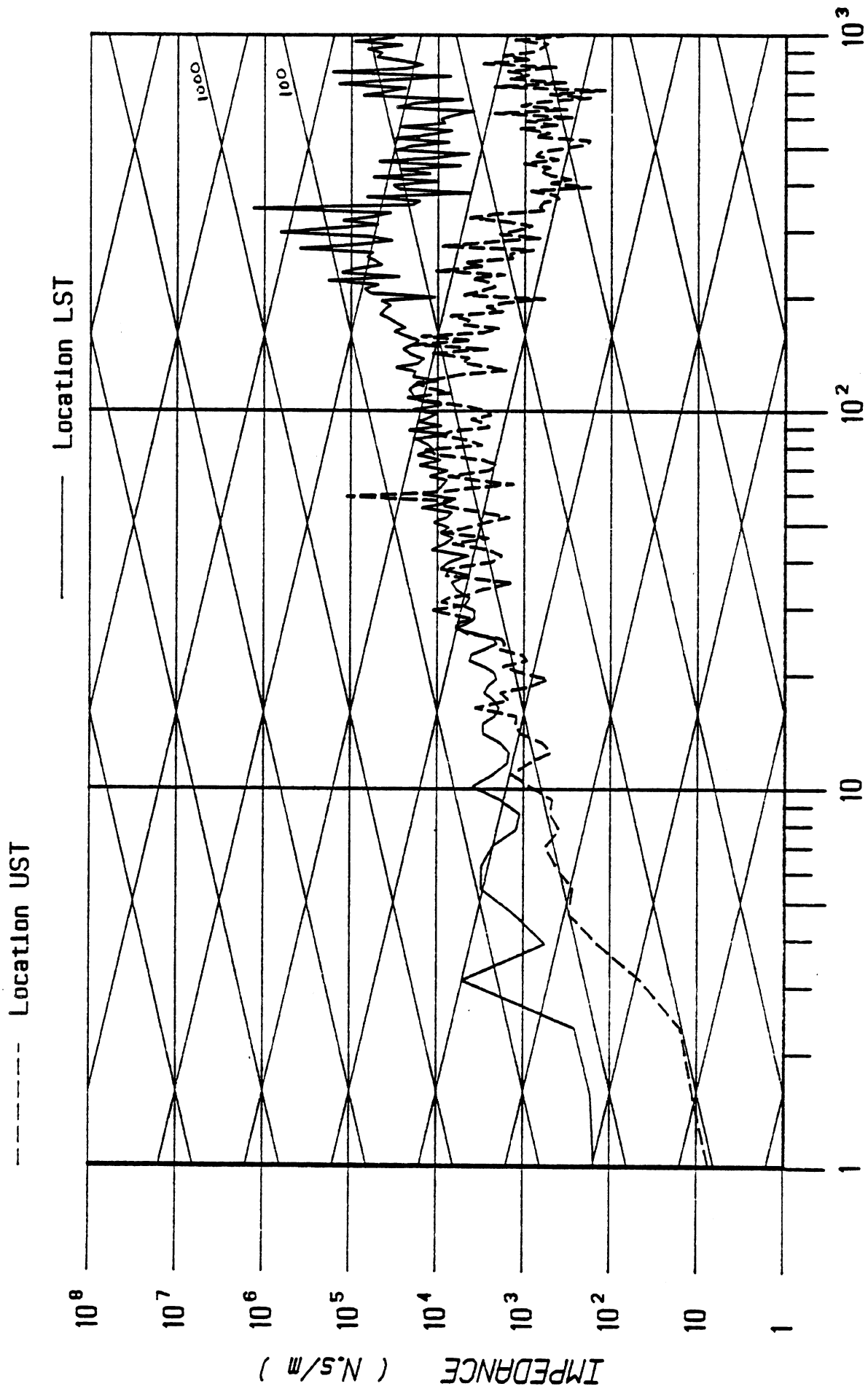
FIGURE 25. IICs for Test T053.
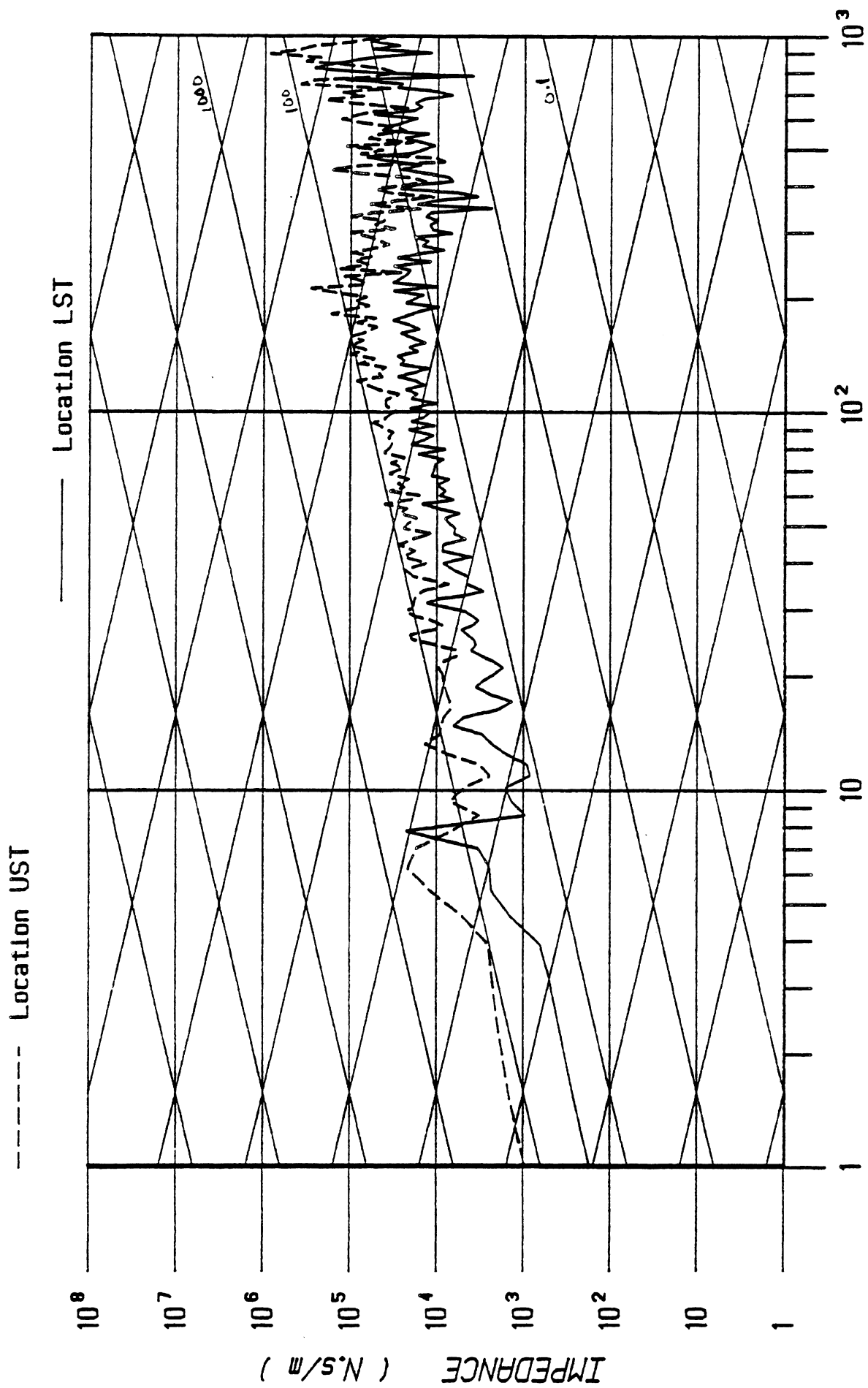
FIGURE 26. IICs for Test T056.

40
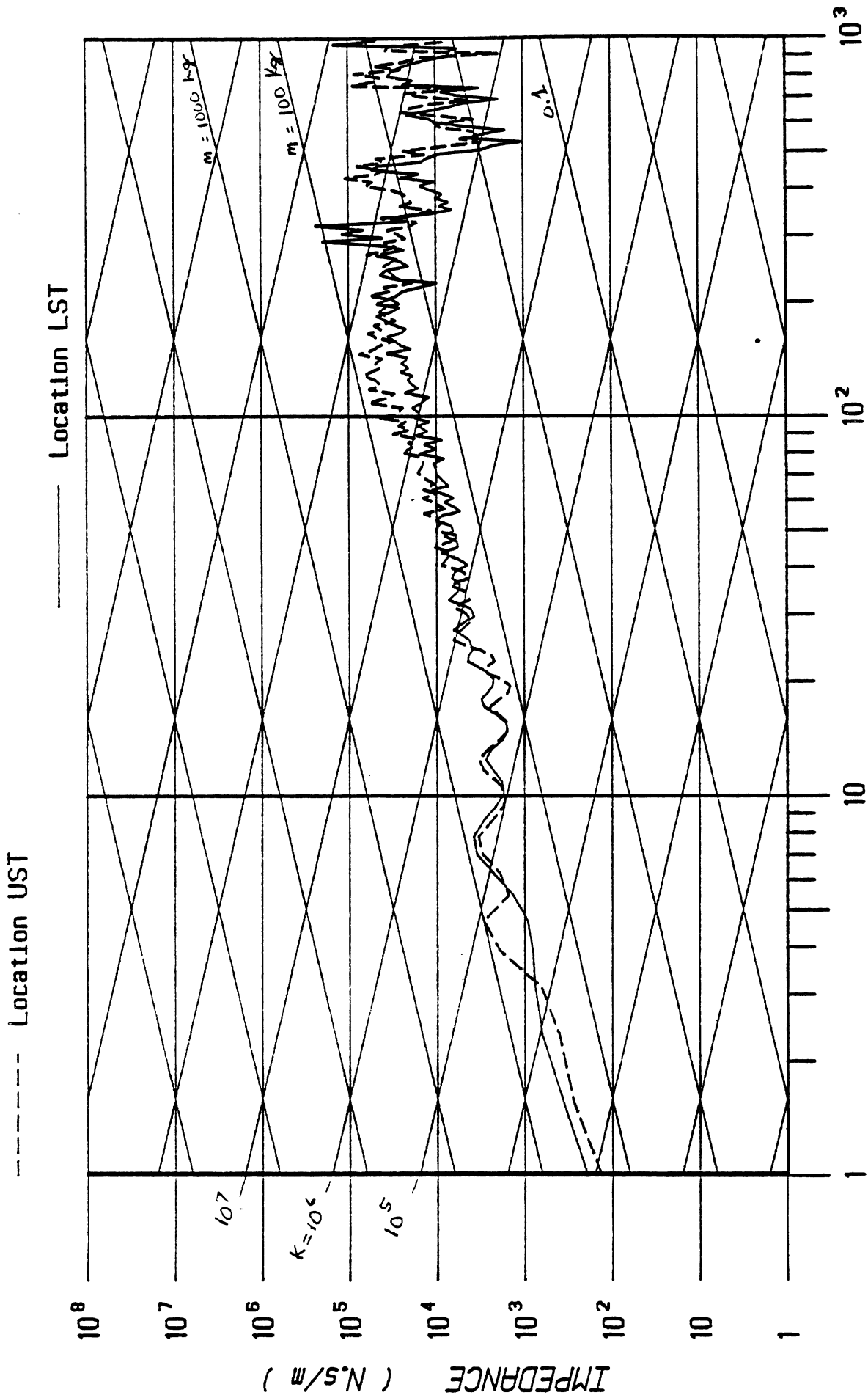
FIGURE 27. IICs for Test T059.

41

FIGURE 28. IICs for Test T062.

42
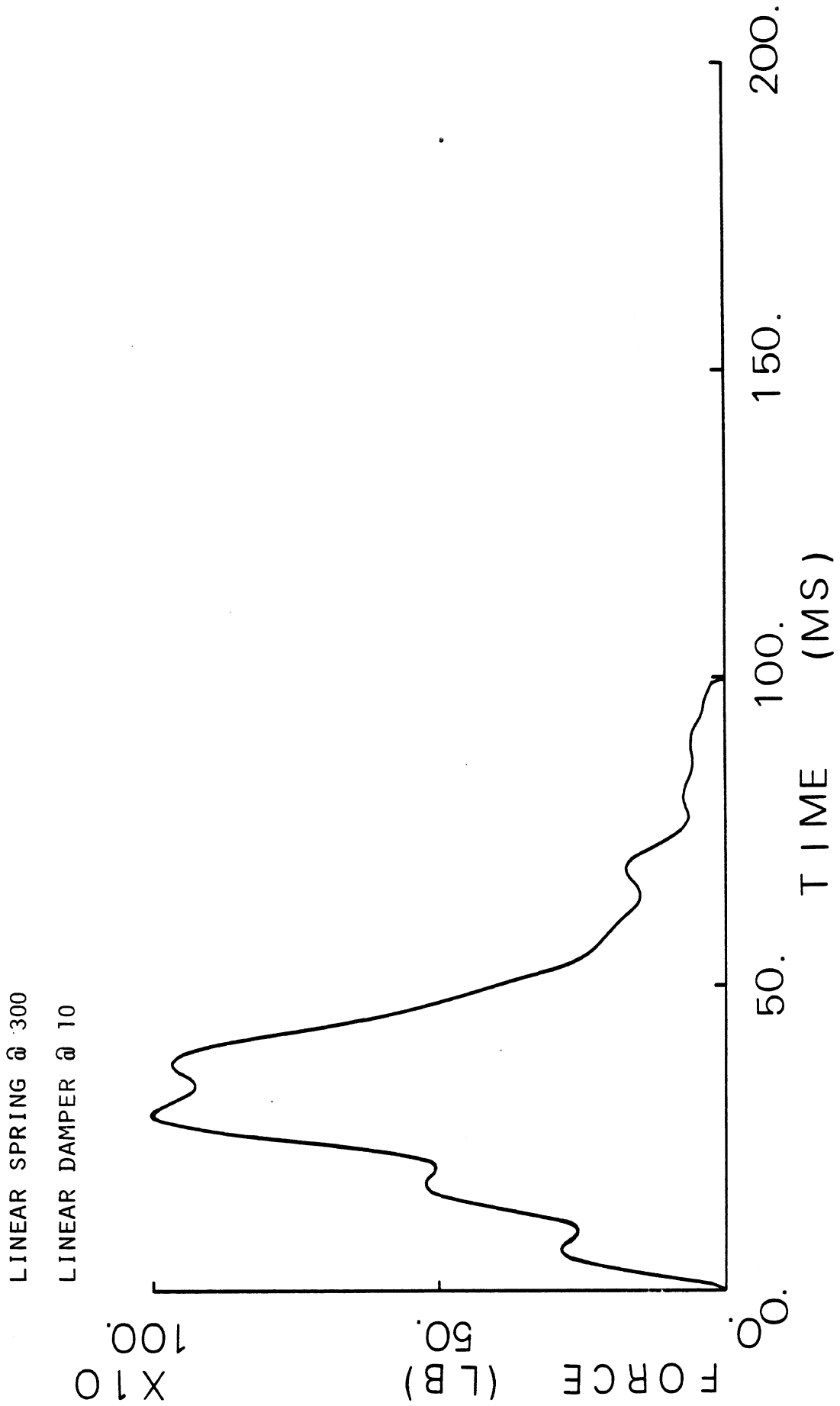
FIGURE 29. Linear spring at 300 and linear damper at 10.

LINEAR SPRING @ 300
LINEAR DAMPER @ 10

FREQUENCY SPECTRUM OF THE PULSE
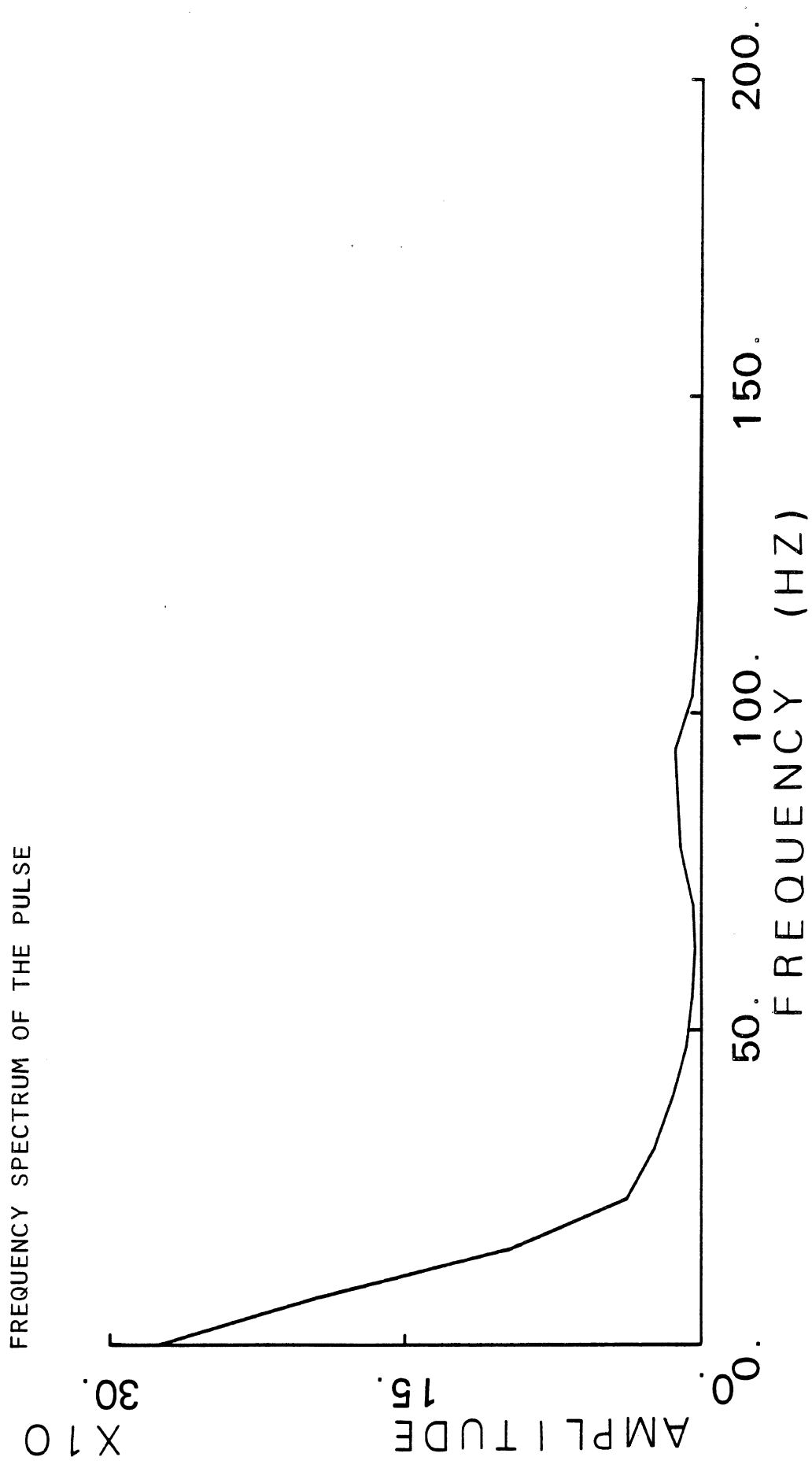
FIGURE 30. Frequency spectrum of the pulse.
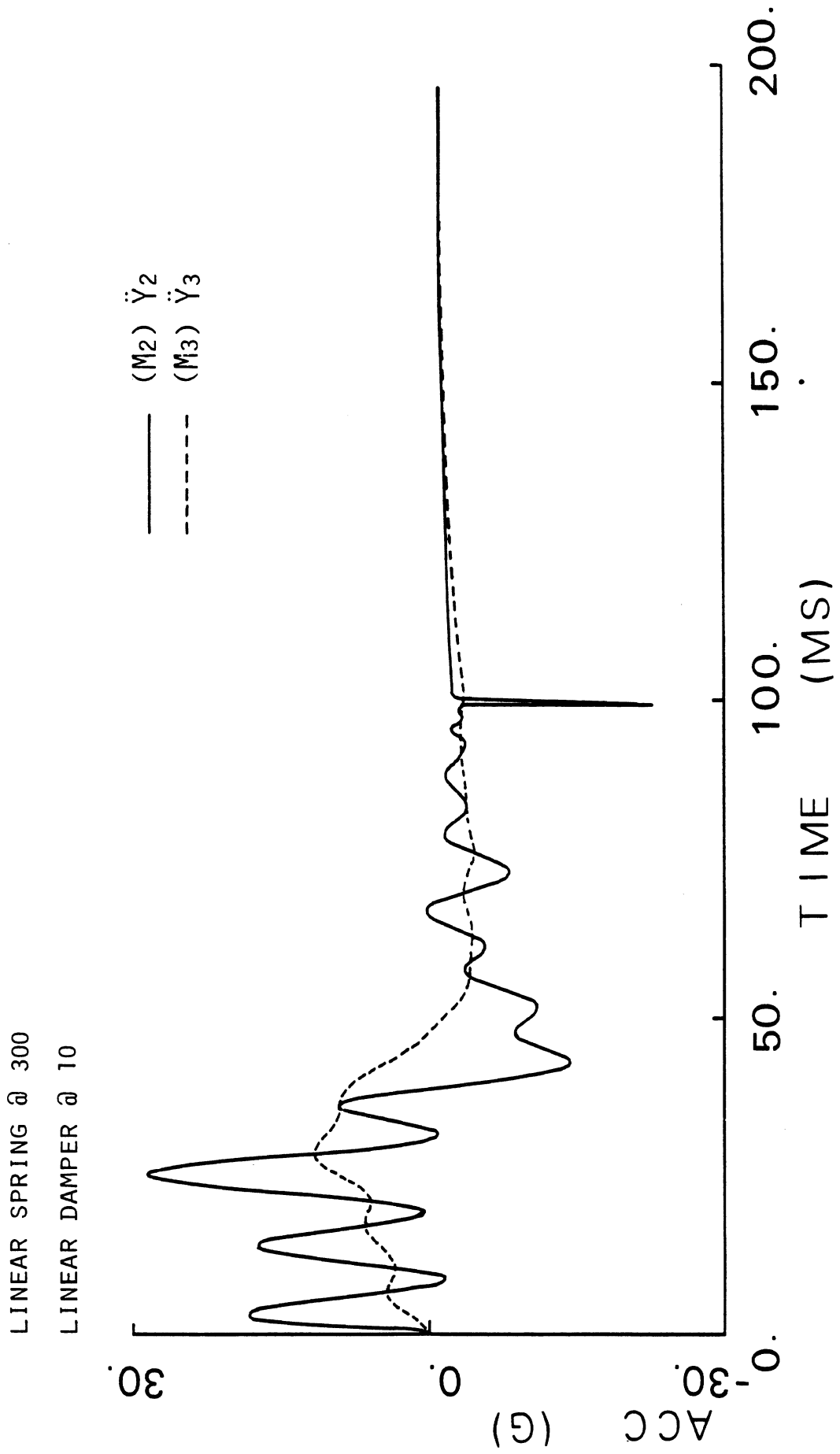
FIGURE 31. Linear spring at 300 and linear damper at 10.

LINEAR SPRING @ 300

BIDIRECTIONAL DAMPER @ 2.3, 12.5

$\ddot{Y}_2$

$\ddot{Y}_3$
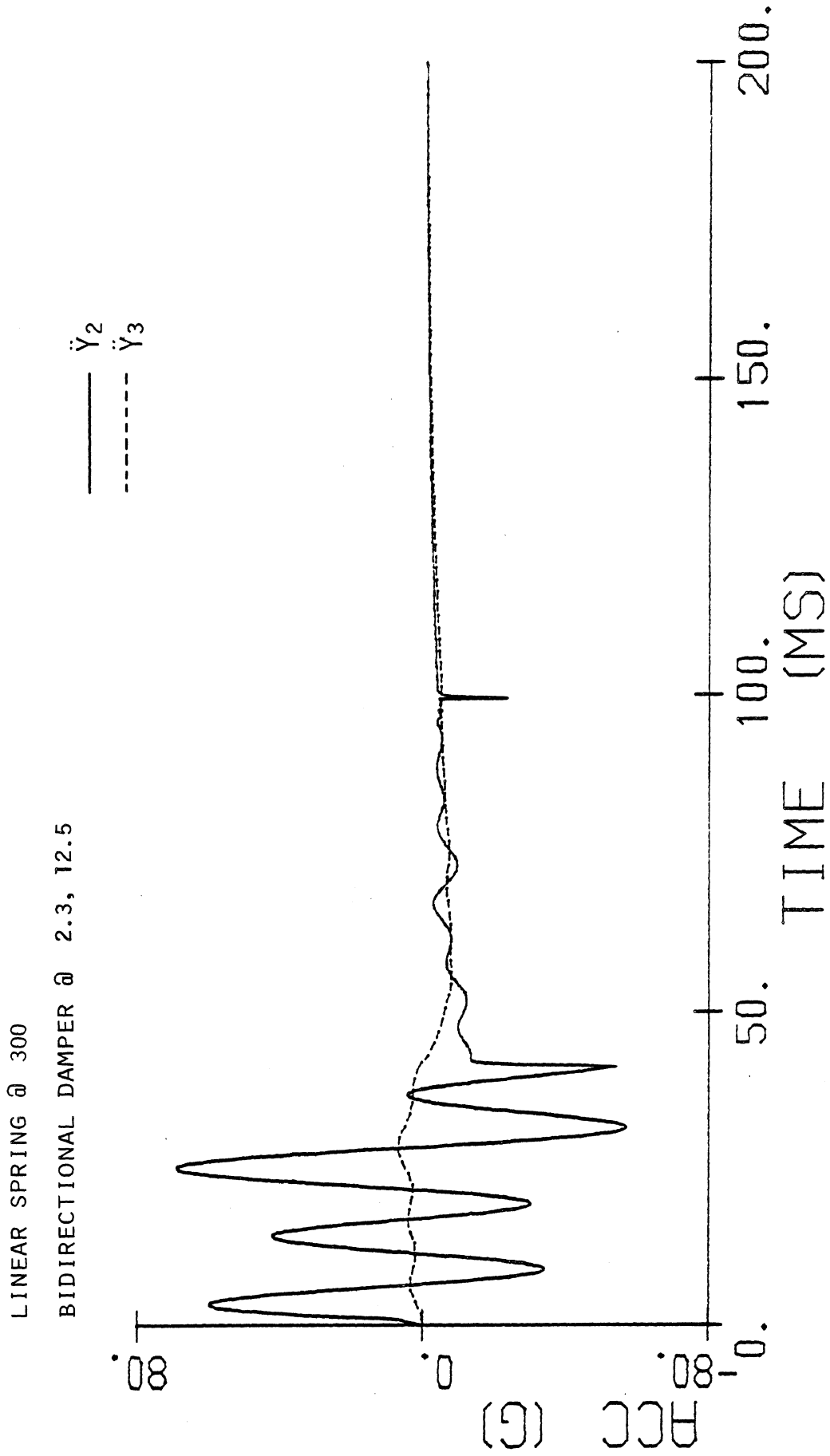
FIGURE 32. Linear spring at 300 and bidirectional damper at 2.3 and 12.5.

TIME (MS)

ACC (G)
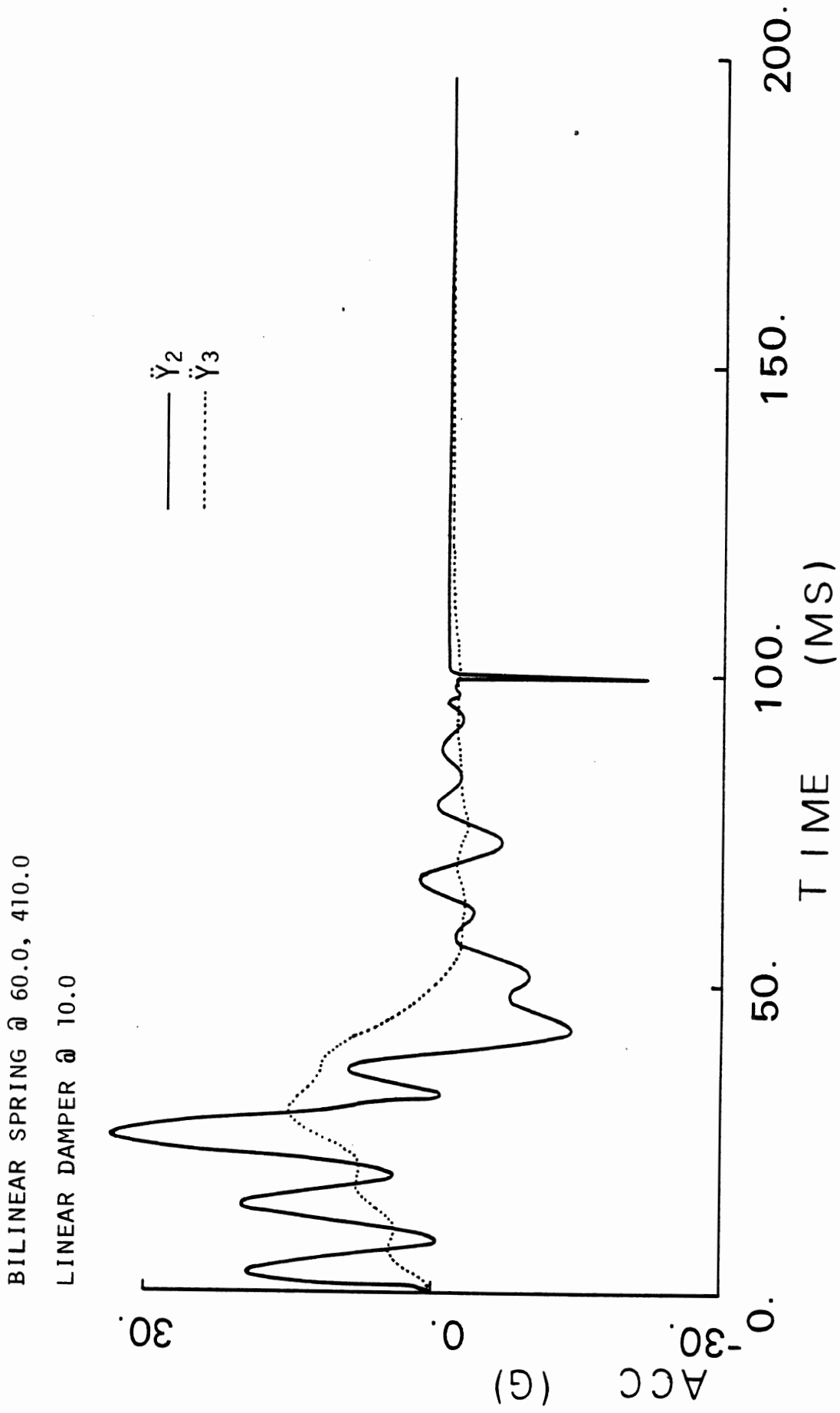
FIGURE 33. Bilinear spring at 60 and 410 and linear damper at 10.

47
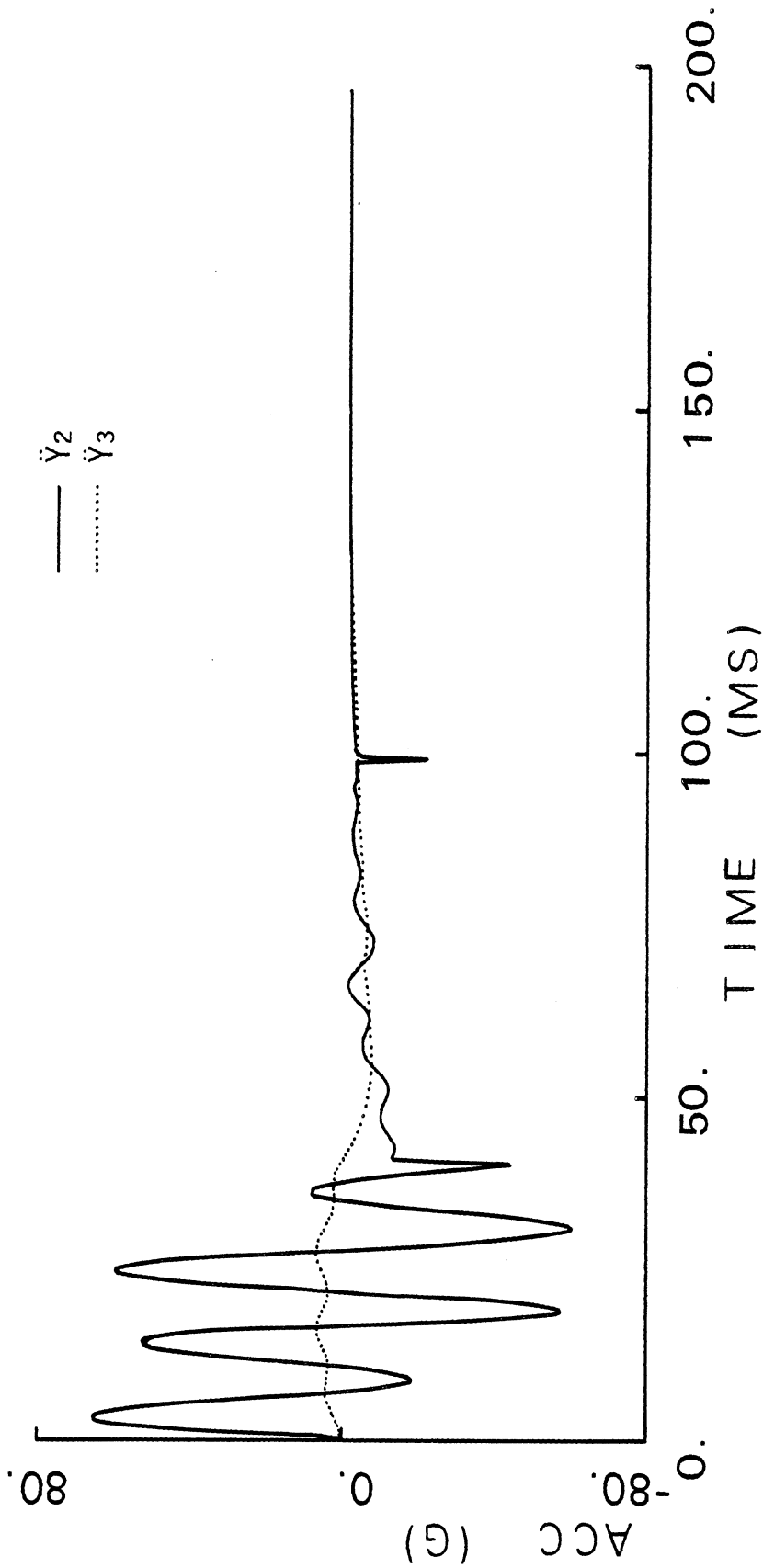
FIGURE 34. Bilinear spring at 60 and 410 and bidirectional damper at 2.3 and 12.5.
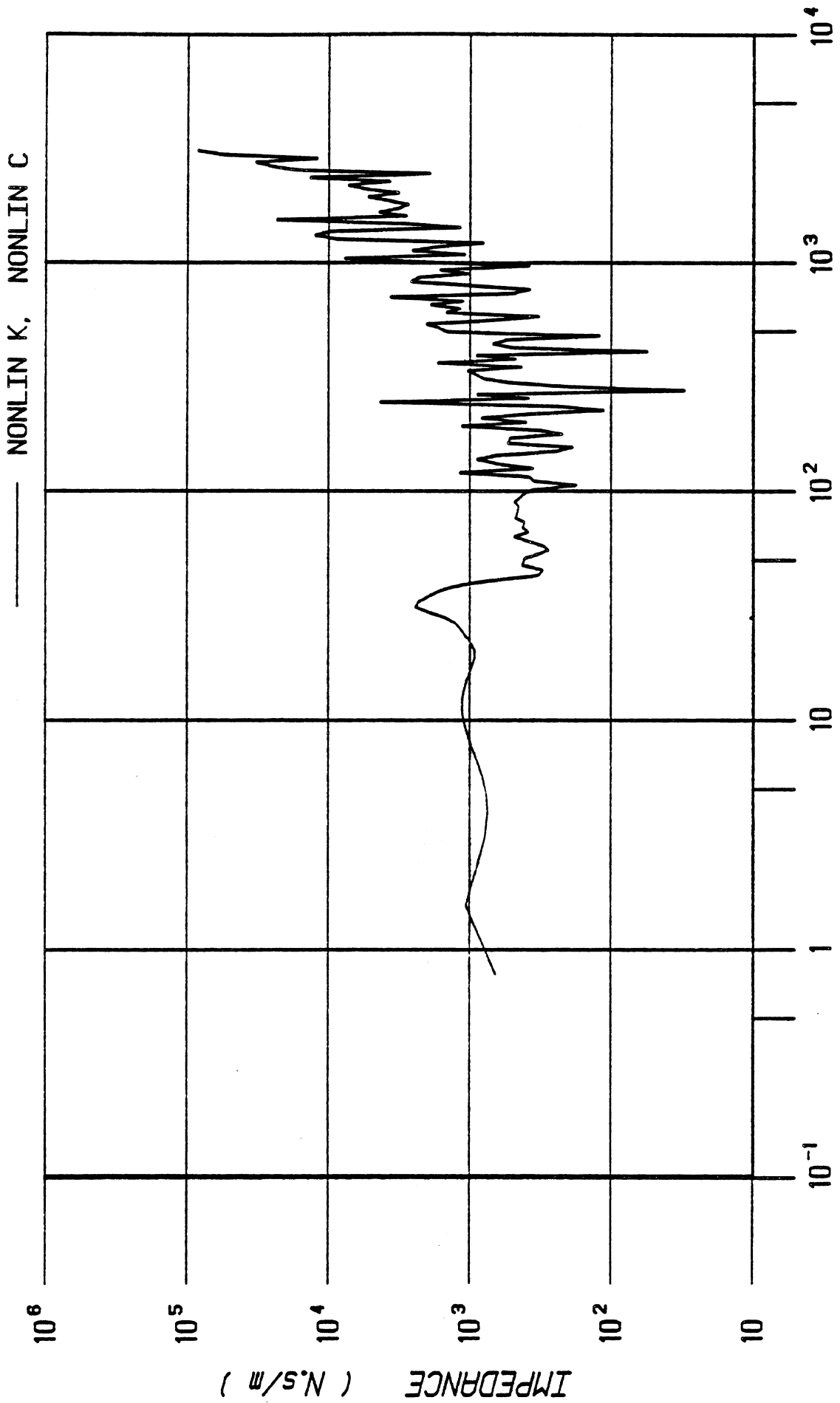
48
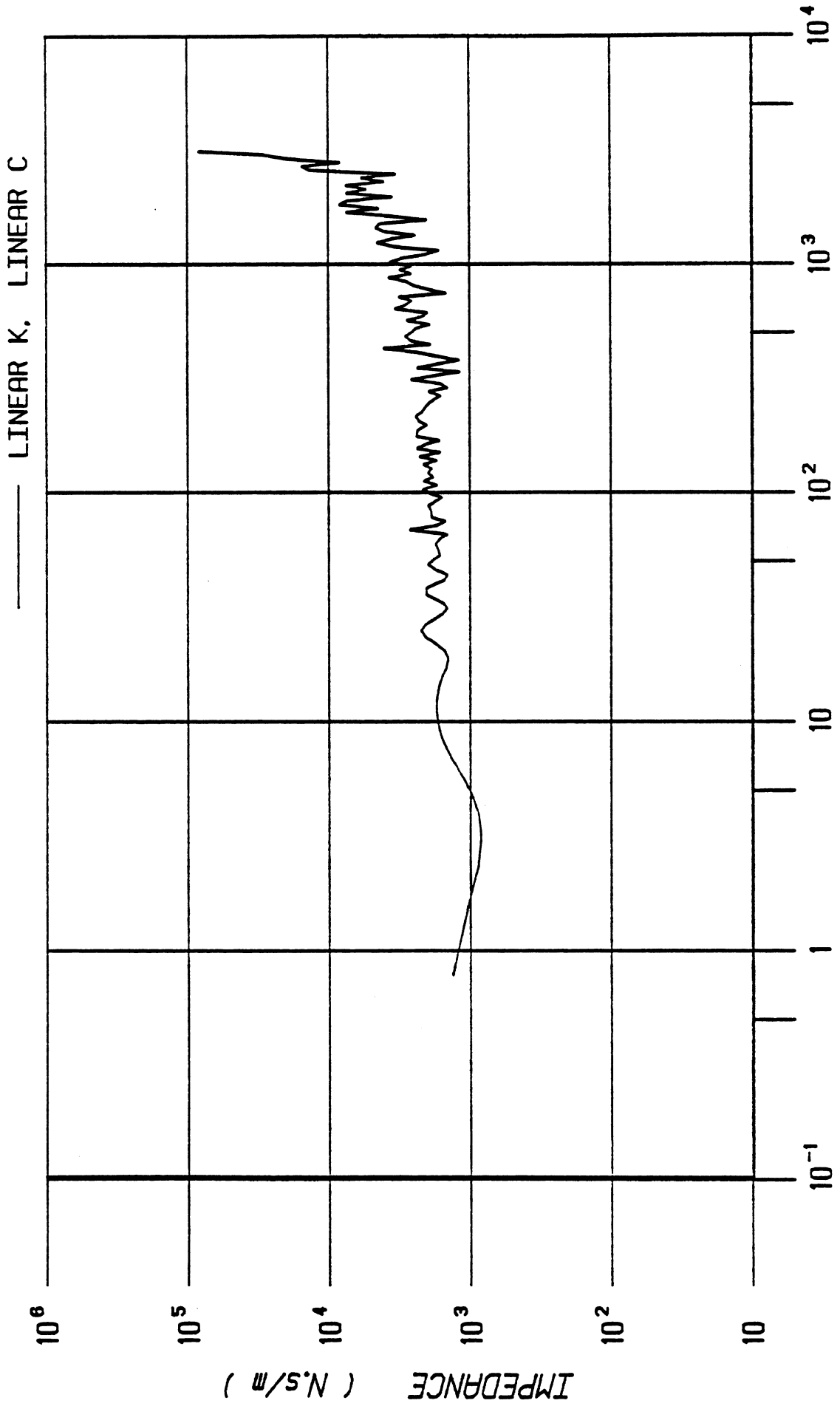
FIGURE 35. Lobdell impact: IZI at M2.
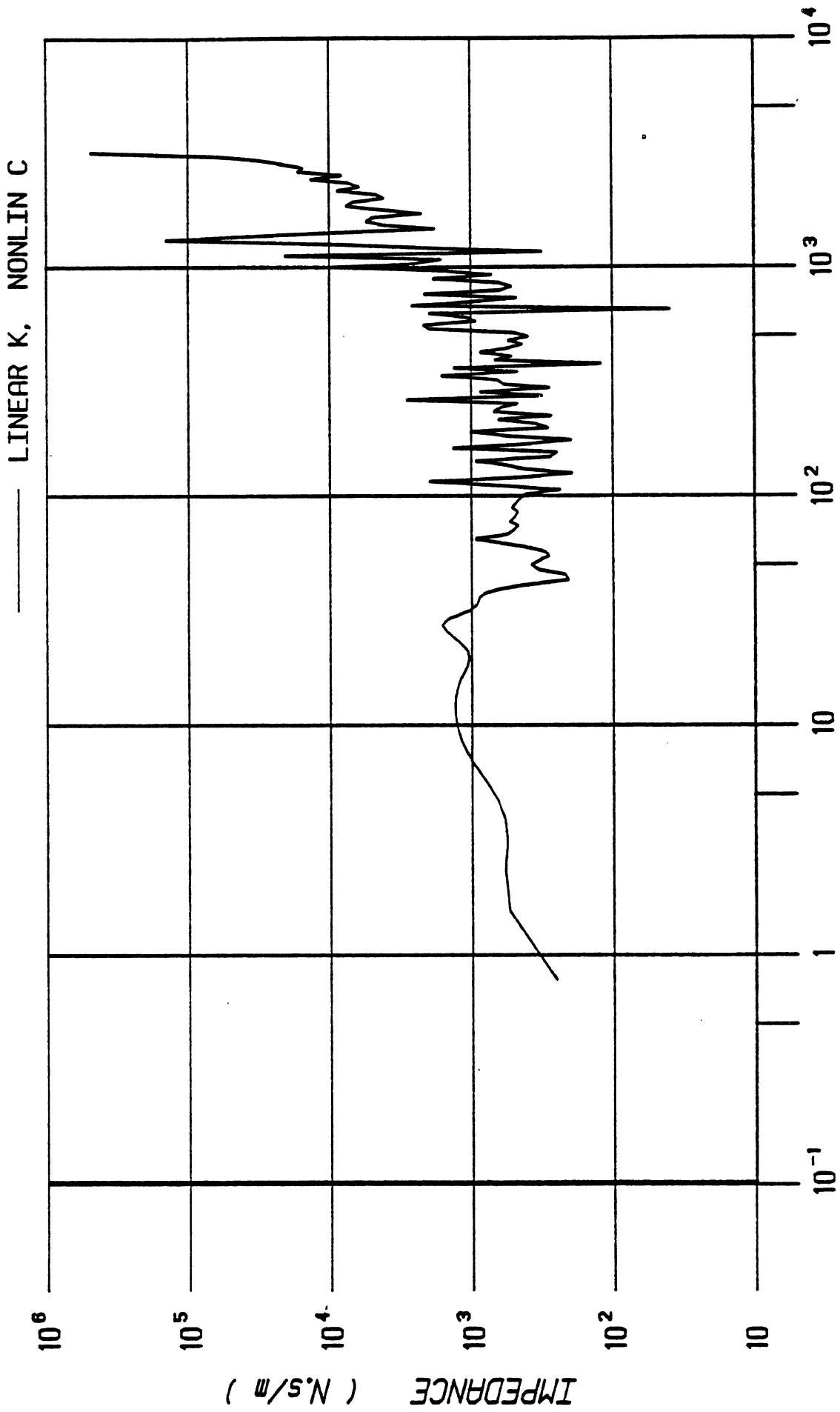
49

FIGURE 36. Lobdell impact: IZI at M2.

FIGURE 37. Lobdell impact: IZI at M2.

51

NONLIN K, LINEAR C

IMPEDANCE (N.S/m)
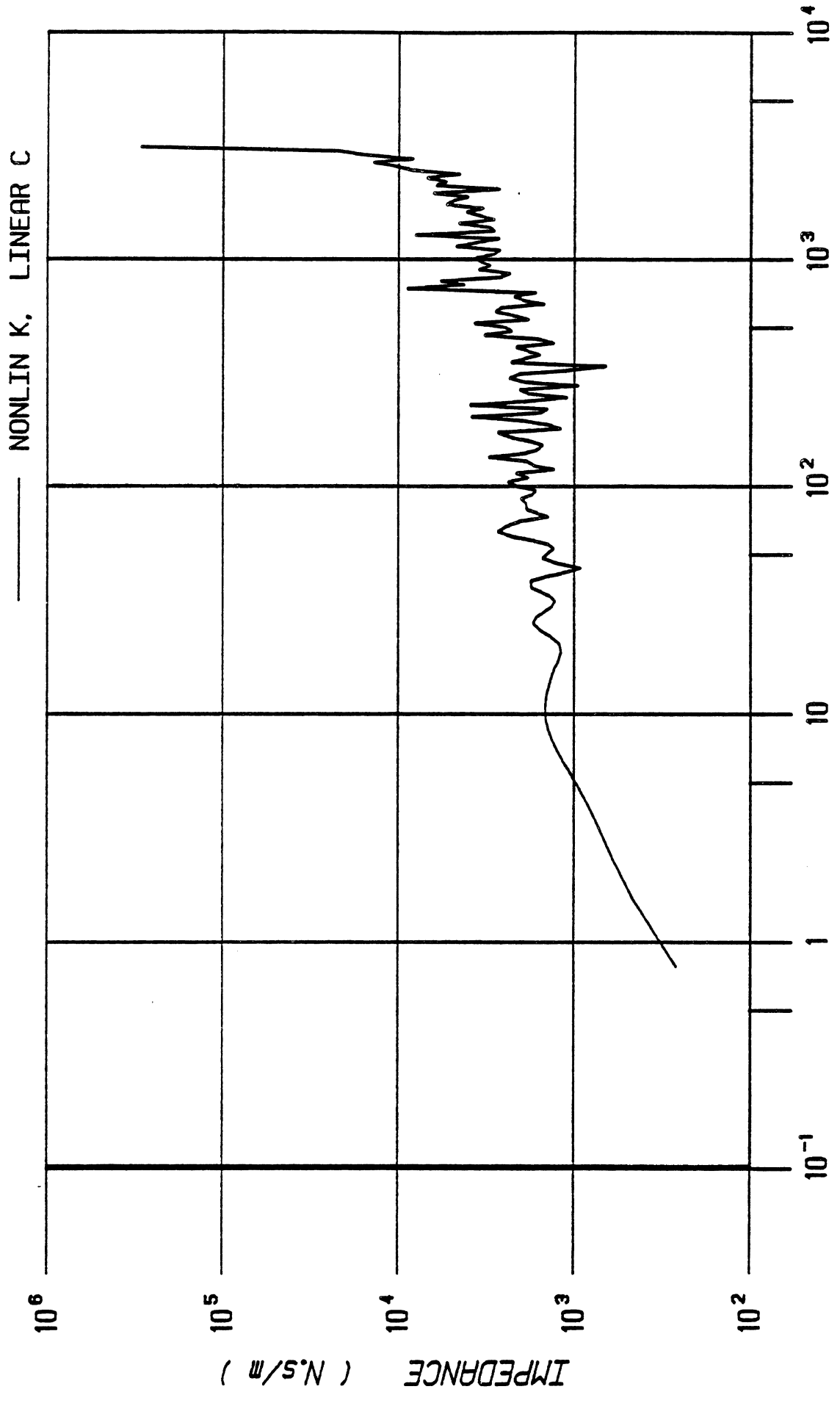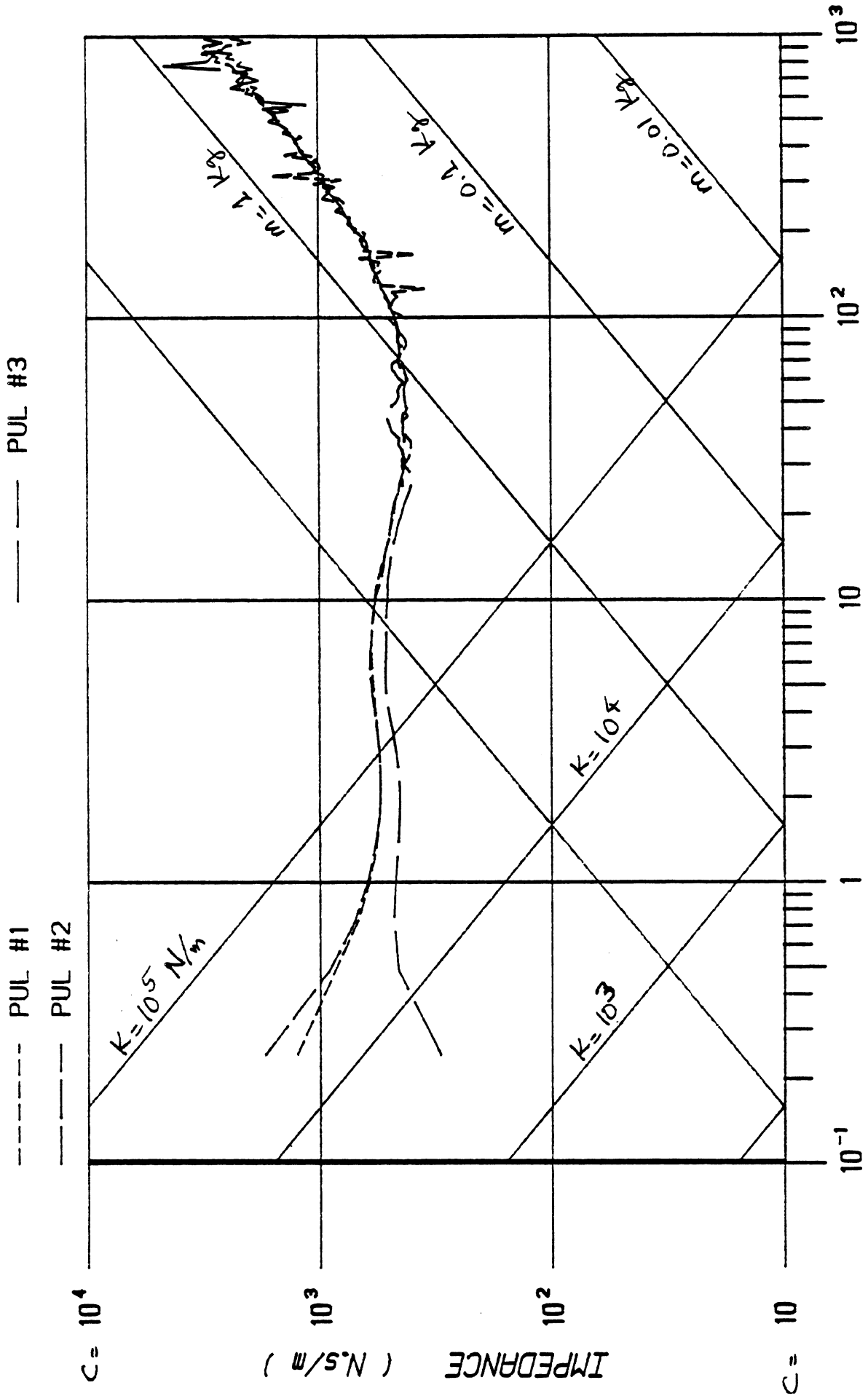
FIGURE 38. Lobdell impact: IZI at M2.

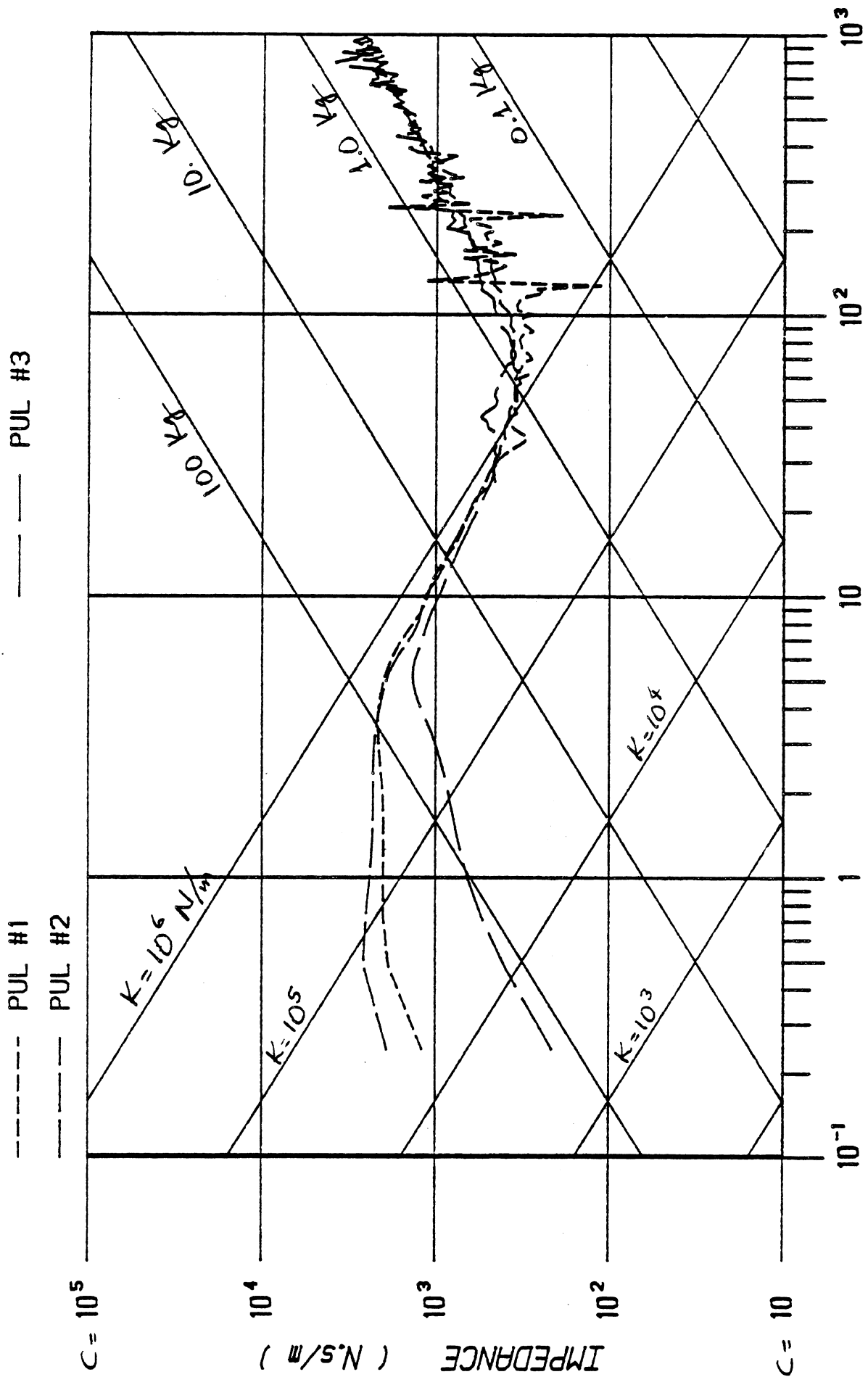FIGURE 39. Linear K23, Z at M2, three impacts.

FIGURE 40. Bilinear K23, Z at M2, three impacts, Lobdell.

54

OTHER REPORTS IN THIS SERIES

OTHER REPORTS

TASK A

INJURY PRIORITY ANALYSIS

Oliver Carsten
James O'Day

PREVIOUS WORK
Overview
The Economic Costs of Injuries
The NHTSA Societal Cost Study
The Harm Model
The Consequences of Injury
The AMA Guides to Permanent Impairment

METHODOLOGY
Overview
Filling in the Gaps in the Chi Data
Translating the Chi Codings into Impairment
Calculating the Present Discount Values
Generating Injury Prioritization from NASS

RESULTS OF THE INJURY PRIORITY ANALYSIS
Overview
The Global Picture
Passenger Car Occupant
Delta V and Clock Direction

COMPARISON OF IPR WITH HARM

CONCLUSIONS

APPENDICES
A: The Medical Panel Meeting
B: Development of a Dependent Variable
for NASS/NCSS Data Analysis
C. Tables at the Occupant Level
D. NASS Codes for Body Region

REFERENCES

TASK B

REVIEW OF BIOMECHANICAL IMPACT RESPONSE AND INJURY IN THE AUTOMOTIVE ENVIRONMENT

John W. Melvin and Kathleen Weber
Editors

HEAD, P. Prasad, J.W. Melvin, D.F. Huelke,
A.I. King, and G.W. Nyquist
    Anatomy of the Head
    Head Injury from Clinical Experience
    Head Impact Response
    Head Injury Mechanisms, Tolerance, and Criteria
    Summary and Conclusions
    References

SPINE, G.W. Nyquist and A.I. King
    Anatomy of the Spine
    Spinal Injury Mechanisms from Clinical
      and Laboratory Experience
    Biomechanical Response of the Spine
    Spinal Injury Tolerance and Criteria
    Summary and Conclusions
    References

THORAX, J.W. Melvin, R.L. Hess, and K. Weber
    Anatomy of the Thorax
    Thoracic Injury from Clinical Experience
    Biomechanical Response of the Thorax
    Thoracic Injury Mechanisms, Tolerance,
      Criteria, and Predictive Models
    Summary and Conclusions
    References
    Appendix: Bibliography of Thoracic Clinical Literature

ABDOMEN, A.I. King
    Anatomy of the Abdomen
    Abdominal Injuries from Clinical Experience
    Abdominal Injury Mechanisms, Tolerance, and Response
    Summary and Conclusions
    References
    Appendix: Bibliography of Clinical Literature
      on Belt-Induced Abdominal Injuries

TASK C

REVIEW OF ANTHROPOMORPHIC TEST DEVICE INSTRUMENTATION, DATA PROCESSING, AND CERTIFICATION TEST PROCEDURES

Rudi H. Arendt
David J. Segal
Richard Cheng

INSTRUMENTATION, R. Cheng
 Force and Moment
 Acceleration
 Pressure
 Flow Measurement
 Deformation Measurement
 Summary

DATA PROCESSING, R. Arendt
 Recommendations
 Review of Data Acquisition and Processing Systems
 Environmental Specifications
 Electronic Design Concept
 Calibration Requirements
 Test Set Characteristics
 References

CERTIFICATION TEST PROCEDURES, D. Segal
 Recommendations
 Review of Existing Dummy Certification Procedures
 Advanced Dummy Certification Testing
 Appendix: Analysis of Certification Testing Procedures

TASK D

REVIEW OF DUMMY DESIGN AND USE

John W. Melvin
D. Hurley Robbins
Kathleen Weber
Kenneth L. Campbell
Joseph Smrcka

TASK E-F

AATD SYSTEM TECHNICAL CHARACTERISTICS, DESIGN CONCEPTS, AND TRAUMA ASSESSMENT CRITERIA

John W. Melvin
Albert I. King
Nabih M. Alem

BIOMECHANICAL DATA BASE
Development of the Data Base
Using Biomechanical Impact Response Data

TECHNICAL CHARACTERISTICS AND DESIGN CONCEPTS
Anthropometry Overview
Head
Spine
Thorax
Abdomen
Pelvis
Extremities
Data Processing
Certification System

TRAUMA ASSESSMENT CRITERIA
Current Trauma Assessment Criteria Recommendations
Data Analyses to Improve Trauma Assessment Criteria

APPENDIX: A FINITE ELEMENT MODEL OF THE HEAD

REFERENCES

TECHNICAL SUPPLEMENTAL REPORTS

PROCESSING OF BIOMECHANICAL DATA FOR AATD DEVELOPMENT

Nabih M. Alem
Richard J. Lehman

FILTER CHARACTERISTICS FOR PROCESSING BIOMECHANICAL SIGNALS FROM IMPACT TESTS

Nabih M. Alem

CHARACTERIZATION OF THE THORAX VIA MECHANICAL IMPEDANCE

Nabih M. Alem
Said Nakhla